

NACA RM E55J12

DECLASSIFIED-AUTHORITY-MEMO.US:  
2313. TAINÉ TO SHAUKLAS  
DATED JUNE 15, 1967

Declassified by authority of NASA  
Classification Change Notices No. 113  
Dated \*\* 6/28/67



NACA

# RESEARCH MEMORANDUM

PRELIMINARY REPORT ON EXPERIMENTAL INVESTIGATION

OF ENGINE DYNAMICS AND CONTROLS FOR

A 48-INCH RAM-JET ENGINE

By George Vasu, Clint E. Hart, and William R. Dunbar

Lewis Flight Propulsion Laboratory  
Cleveland, Ohio

FACILITY FORM 602

N67-31545

(ACCESSION NUMBER)

65  
(PAGES)

(THRU)

1  
(CODE)

(NASA CR OR TMX OR AD NUMBER)

28  
(CATEGORY)

THE  
of the  
manner to an unauthorized person is prohibited

## NATIONAL ADVISORY COMMITTEE FOR AERONAUTICS

WASHINGTON

March 16, 1956

GROUP

DOWNGRADING 12 YEAR  
INTERVALS: NOT AUTOMATICALLY DECLASSIFIED

## NATIONAL ADVISORY COMMITTEE FOR AERONAUTICS

RESEARCH MEMORANDUM Declassified by authority of BAS1  
Classification Change Notices to. 113  
Dated \*\* 6/28/67

## PRELIMINARY REPORT ON EXPERIMENTAL INVESTIGATION OF ENGINE

## DYNAMICS AND CONTROLS FOR A 48-WCH RAM-SET ENGINE

By George Vasu, Clint E. Hart, and William R. Dunbar

## SUMMARY

The preliminary results of an experimental investigation of engine dynamics and controls for a 48-inch ram-jet engine are presented. The investigation was conducted in a free-jet facility at a Mach number of 2.76 and altitudes from 68,000 to 82,000 feet.

The engine data presented include steady-state performance, indicial response, frequency response, and ignition characteristics. Transient and frequency-response data were found to yield approximately the same information on the nature of the engine dynamics. The predominant engine dynamic characteristic for pressures to fuel flow was dead time, with values ranging from 0.018 to 0.053 second for static pressures, depending primarily on the distance of the pressure tap from the burning zone.

Ignition data are presented for representative fuel-air ratios which show that the normal shock overshoots its final position by several feet during ignition transients.

Four control systems of the same general type but differing in the location of the tap for the controlled pressure were investigated; typical data are presented for one of the systems. All the systems were designed to maintain a constant ratio of a diffuser static pressure to a reference static pressure on the engine-inlet cone. The data presented for the one control show that such operation results in very nearly constant diffuser total-pressure recovery over a range of altitudes.

Data on the engine-control-system response time and percent overshoot to fuel-flow step disturbances are presented for a broad range of control settings. All the fuel step disturbances were large enough to have placed the engine in the subcritical buzz region without control. However, the control response was fast enough for all control settings investigated to prevent subcritical operation. For the range of control settings studied, response times from 0.08 to 0.5 second were obtained.

The response time was also found to be essentially independent of disturbance size for fuel-flow disturbances from 2130 to 4260 pounds per hour (13.6 to 27.2 percent of fuel flow at max. recovery).

## INTRODUCTION

The role of the ram jet as a propulsion device has become more prominent in recent years as a result of the emphasis placed on guided missiles and aircraft that operate at high supersonic Mach numbers. In order to fully utilize the capabilities of the ram-jet power plant, suitable engine control systems must, of course, be developed. Analyses made several years ago at the NACA Lewis laboratory have indicated parameters suitable for ram-jet control and have suggested methods for controlling the engine using these parameters (refs. 1 and 2). A program was also instituted for the experimental investigation of engine dynamics and control systems on a 16-inch ram-jet engine in the 8- by 6-foot supersonic wind tunnel. Some of the results of that research are reported in references 3 to 5.

More recently, an investigation of engine dynamics and controls for a 48-inch ram-jet engine has been made. This investigation was part of an over-all program to evaluate the altitude performance of the ram-jet engine in a Mach 2.76 free-jet facility. The purpose of the controls phase of this program was to determine the dynamics of a large ram-jet engine, to obtain detailed information on normal shock movement and gas dynamics within the diffuser, and to determine how close to critical recovery controls could operate the engine and still provide satisfactory steady-state and dynamic operation for a range of altitudes. The control systems investigated were closed-loop diffuser pressure controls with altitude and some Mach number compensation.

This preliminary report presents a brief coverage of the data obtained on the 48-inch ram-jet engine during the engine dynamics and controls phase. All the data presented herein are for a Mach number of 2.76, altitudes from 68,000 to 82,000 feet, and an engine-inlet temperature of 528° F. The data include engine characteristics pertinent in controls work and information on one of the four control systems investigated. The engine data contain steady-state performance, indicial response, frequency response, and ignition characteristics. The controls data also cover both steady-state and dynamic performance, and indicate the kind of performance to be expected from the type of controls investigated.

## APPARATUS AND INSTRUMENTATION

The apparatus and instrumentation used in the investigation consist of the ram-jet engine, the free-jet facility, an electrohydraulic fuel servo system capable of high-frequency performance, instrumentation for dynamics studies, and an analog computer utilized as a flexible control. This equipment is discussed in detail in the following sections.

## Engine

Diffuser. - A phantom sketch of the diffuser is shown in figure 1(a). The inlet portion was, essentially, a  $216^\circ$  segment of a single-cone ( $22^\circ$  half-angle) Ferri type diffuser designed for a flight Mach number of 2.76.

In order to improve the combustor-inlet velocity profile and to avoid flow separation, a screen was installed across one-half of the diffuser outlet. This screen comprised a square array of 1/4-inch rods and blocked 20 percent of the (half) area. Details on diffuser performance are presented in reference 6.

A side view of the diffuser indicating the location of transient instrumentation is shown in figure 1(b). (Symbols are defined in appendix A.) Pressure pickups 1 to 11 were connected to static taps located along the top of the innerbody, 2 inches off-center, as shown in the cross-sectional sketch of figure 1(b). Tap 12 was located at 4:00 o'clock looking downstream, and tap 20 was located at the top of the inlet cone well forward of the engine inlet. Pickup 14 was connected to a total-pressure probe at the station of the cowl lip.

The area variation through the diffuser is shown in figure 2.

Combustor. - The transition from the 32-inch-diameter diffuser outlet to the 48-inch-diameter combustion chamber was accomplished with a  $30^\circ$  included-angle conical-diffuser section in which the flameholder and the fuel-injection system were mounted. The length of the combustion chamber from the downstream end of the transition section to the beginning of the nozzle was  $6\frac{1}{2}$  feet. The cross section of the combustor is shown in figure 3(a), and a cutaway view is shown in figure 3(b).

Fuel was injected normal to the main air stream by means of simple orifices in sixteen 1/2-inch-diameter radial tubes, equally spaced circumferentially, and supplied from a common external manifold. Three such systems, consisting of three separate manifolds, each supplying 16 radial tubes, were installed to facilitate a study of fuel-distribution effects on burner performance. The three systems were designated

according to location as either upstream, intermediate, or downstream. During the controls investigation, fuel was injected through only two of the three systems; and the size and location of the orifices in the spray bars were designed to give an even fuel distribution, that is, equal fuel flow per unit of area. Figure 3 shows a typical fuel bar installed in the combustor.

The fuel used throughout the investigation was MIL-5624B, grade JP-5, with a lower heating value of 18,625 Btu per pound.

Ignition was achieved through the use of two surface-discharge spark plugs located in the pilot annulus. A separate power system of the condenser-discharge type was used to supply each plug.

Instrumentation details for the combustor are shown in figure 3(a).

Information on combustor performance, as well as further details of combustor design, is contained in references 7 and 8.

Exhaust nozzle. - The convergent-divergent exhaust nozzle had a throat area 54.6 percent of the combustion-chamber area with a convergent section of  $25^\circ$  half-angle and a divergent section of  $12^\circ$  half-angle.

### Facility

The ram-jet engine was tested in a free-jet facility. The starting and performance characteristics of the free-jet facility are reported in reference 9. A schematic diagram and cutaway drawing of the engine installation in the facility is shown in figures 4(a) and (b), respectively. Dried and heated air from the facility air system entered the supersonic nozzle and was accelerated to a Mach number of 2.76. Approximately 52 percent of the air entered the engine diffuser, while the remaining air passed through the jet diffuser into the facility exhaust system.

### Fuel Servo System

An electrohydraulic servo system was specially designed to provide the fast response required for ram-jet dynamics and controls investigations. This system controlled the flow to the upstream set of spray bars. The flow to the intermediate set was controlled manually. (The downstream set of spray bars was not used during the controls investigation.)

The operation of the fuel servo system is discussed in appendix B.

3751

The steady-state performance of the system is shown in figure 5, where the fuel flow is shown to be a linear function of servo input voltage. The dynamic performance of the system, as installed for the test program is shown in figure 6, where the frequency response is presented for fuel-valve position to servo input voltage  $\Delta V_f / \Delta V_i$ , fuel flow (fuel nozzle pressure drop) to servo input voltage  $\Delta w_{f,u} / \Delta V_i$ , and fuel flow to fuel-valve position  $\Delta w_{f,u} / \Delta V_f$ . The frequency-response characteristic includes the effects of all the necessary piping required for the installation. The phase shift was  $180^\circ$  at 36 cps, and the amplitude response was down less than 20 percent up to approximately 50 cps. The dynamic performance attainable with this system makes it very suitable for ram-jet dynamics and controls studies.

### Instrumentation

Gas-pressure sensors. - For transient pressure measurements, three types of variable inductance pickups were used. These were designated types I, II, and III. Type I was characterized by its small size, diaphragm construction, high natural frequency, and rather low output voltage. Types II and III were two models of the same make and were characterized by twisted-tube construction, high natural frequency, relatively high output voltage, and better accuracy (lower drift and better linearity) than type I. All pressure pickups were installed in water-cooled jackets to maintain operation within the designed temperature range. Connecting tube lengths were kept to a minimum to ensure the fastest possible response; the inside diameter of the tubing was 0.040 inch, which gives a reasonable amount of damping.

Typical frequency-response characteristics for pickup types I, II, and III are shown in figures 7, 8, and 9, respectively. These data were obtained from bench tests of the sinusoidal response of each type transducer and associated tubing. For each engine variable measured, the type of transducer used and other pertinent information are tabulated in table I. For most of the pickups, the tubing length and diameter were the same (9 in. of 0.040-in.-I.D. tubing); and for the engine dynamics phase all the static-pressure pickups were the same type (type I). For the controls phase, where good accuracy (low drift and good linearity) is very important, pickups 4, 5, 6, 10, and 20 were changed to either type II or III.

Diffuser pressure recovery was obtained from a total-pressure rake at station 653.2.

Manometers were used for pressure measurements during steady-state operation.

3

Fuel-pressure sensors. - An indication of the amount of fuel flow to the engine was obtained by measuring the pressure drop across the orifices in the spray bars. A resistance, strain-gage, differential pressure pickup was connected to a line between the manifold and a spray bar to measure upstream and intermediate fuel flows. These pickups were referenced to the combustion-chamber air pressure near the spray bars. From bench tests the response of the fuel-pressure side of the pickups with associated tubing was found to be essentially flat to at least 150 cps with no measurable phase shift.

For steady-state measurements the fuel flow was measured by connecting manometers to indicate the pressure drop across an orifice in the fuel line.

Fuel-valve position. - The fuel-valve position was sensed by a linear variable differential transformer. The signal was then amplified, demodulated, and filtered, giving a d-c signal proportional to the fuel-valve position.

Amplifiers. - The pressure variables were amplified by carrier-type amplifiers. Fuel-valve position and fuel servo input voltage were amplified with d-c amplifiers. The carrier amplifiers are shown in racks 1 and 3 of figure 10 and the d-c amplifiers in rack 5.

Recording equipment. - All transients were recorded on sensitized paper with oscillographs using galvanometers with natural frequencies of 200 to 500 cps. For monitoring purposes certain variables were also recorded with direct-inking strip-chart recorders.

The photographic oscillographs are shown in racks 2 and 4 of figure 10, and the direct-inking recorder in rack 7.

### Computer

For the controls investigation, the necessary computation was performed by an electronic differential analyzer, which is shown in rack 6 of figure 10. The computer performs the required operations through the use of high-gain d-c operational amplifiers and associated plug-in input and feedback impedances. The output of the computer was fed into the fuel servo control chassis, which is located in rack 5.

## DESCRIPTION OF CONTROL

### Parameters Used

For the control systems investigated, static pressures along the diffuser innerbody were chosen as the control pressures. In order to

determine the effect of tap location on control performance, four systems were investigated, each with a different location of the control pressure tap. Stations 502, 517, and 532, which are well forward in the diffuser near the minimum-area section (fig. 1(b)), were chosen for three tap locations. The controls using these pressures were designed to place the normal shock at the control pressure tap. The object was to try, in succession, control systems using  $p_{532}$ ,  $p_{517}$ , and  $p_{502}$  to see how far forward the normal shock could be positioned and still maintain satisfactory performance.

For the fourth control system, a tap location near the diffuser exit (station 622) was chosen for the controlled pressure. Although this system could be designed to operate the engine over a rather broad range, it was set to hold the normal shock in about the same position as the  $p_{532}$  control. The object was to compare the performance of this system using a pressure near the diffuser exit with those systems using pressures well forward (near the inlet).

Static pressures were chosen because they usually provide a better control signal than total pressures. Their dead time in response to disturbances is generally shorter, and the accuracy attainable with a single tube is better.

In each case the control system was referenced to a static pressure well forward on the surface of the inlet cone (station 429). This reference pressure was chosen primarily because it affords not only altitude compensation, but also some Mach number compensation. The variation with diffuser recovery of the ratio of each of the controlled pressures to the reference pressure is shown in figure 11. Since ratios are involved, the curves generalize for a range of altitudes.

The circles show the operating points chosen. Each point for pressures 502, 517, and 532 was somewhat arbitrarily chosen to give operation at a pressure midway between the minimum value which would exist at low recovery and the maximum attainable during the investigation (at 0.63 recovery). A convenient method of attaining more rapid responses for disturbances which would tend to drive the engine subcritical than for disturbances in the other direction would be to choose an operating point nearer the low end of these characteristics. The signal available to the control would then be larger for disturbances which increase these pressures than for those which decrease them.

The point shown for  $p_{622}$  gives operation at essentially the same recovery as chosen for  $p_{532}$ . This recovery was felt to offer a considerable margin from the peak recovery to ensure safe operation over a range of altitudes and for various disturbances.

The location of the desired operating point on each of these characteristics determines the factor that must be applied to the reference pressure to give proper control operation. For example, for  $p_{532}$  the point at a ratio of  $p_{532}/p_{429}$  of 3.10 indicates that  $p_{429}$  must be multiplied by 3.10 before it is compared with  $p_{532}$  in the control.

### Block Diagram of Control

The manner in which the controlled and reference pressures were connected to the control and then back to the engine through a fuel servo is shown in figure 12. At the engine, the controlled pressure was sensed, then amplified. In a similar manner the reference pressure was sensed and amplified. Before being compared, the controlled and reference pressure signals were properly scaled to attain the factor desired as indicated previously in figure 11. The signals were then compared and the error fed to a control.

In general, a proportional-plus-integral control was used. Previous analysis based upon the engine dynamic characteristics indicated that this type of control is desirable.

The output of the control was then connected to the fuel servo which, in turn, varied the fuel flow to the engine, thus affecting the controlled pressures.

The details of the circuitry from the outputs of the carrier amplifiers to the servo input are shown in figure 13. The electronic differential analyzer shown in rack 6 of figure 10 was used for this portion of the control system. The drift, linearity, and accuracy of the sensors, amplifiers, and computer portion of the control systems were such that errors due to these factors were negligible. The sensors, amplifiers, and circuitry for the controlled and reference pressures were matched as closely as possible so that temperature effects or other minor effects on components in the controlled pressure branch would be cancelled to a certain extent by the action of the corresponding components in the reference pressure branch.

### PROCEDURE AND RANGE OF VARIABLES

The program for the 48-inch ram-jet engine consisted of two parts, an investigation of engine characteristics pertinent to control design and an investigation of the four control systems. The procedure for these two parts of the investigation is discussed in the following two sections.

### Engine Investigation

In the engine phase of the investigation, several types of data were taken: steady-state, indicial response (response to step disturbances), frequency response, and ignition data.

Steady state, indicial response, and frequency response. - Steady-state, indicial-response, and frequency-response data were taken in the usual manner. Details on the procedure used are discussed in some of the earlier NACA reports (e.g., ref. 3).

Ignition. - In order to obtain ignition data, first the engine-inlet pressure was adjusted to give a satisfactory altitude for starting the engine. Next, a certain fuel-air ratio was set up by means of an adjustable fuel valve. After the proper fuel-air ratio was set, the fuel flow was turned off by closing a solenoid shut-off valve, leaving the main adjustable fuel valve set to the proper position for the desired fuel flow. Several minutes were then allowed for the air to clear the engine of any excess fuel that might have accumulated. Following this purging period, the solenoid shut-off valve was opened, allowing the fuel flow to rise rapidly to the preset value. When the fuel flow reached the proper value, the ignition system was energized, causing the fuel to ignite. After the engine was lighted, the ignition was turned off. The oscillograph recorders were turned on just before the shut-off valves were opened, and turned off after the ignition transient settled out. Ignition data were taken at increasingly richer fuel-air ratios until finally the normal shock was expelled from the diffuser on the last transient.

### Controls Investigation

Steady state. - The first phase of the controls investigation consisted of operating the control in steady state over a range of altitudes. The procedure used to accomplish this follows. First, sensors, amplifiers, computer, and so forth, had been previously calibrated and the proper settings for the control were inserted. Next, a suitable altitude for ignition of the engine was set, and the engine was lighted with the fuel flow set manually. As soon as the engine ignited, the fuel flow was set somewhere near the control point, and the control was switched to automatic. The control then automatically increased the fuel flow to the proper value for the control point.

Once on automatic control, the altitude was varied over the complete range to check the steady-state performance of the system.

Dynamics. - The next phase of the controls investigation was to add a step voltage to the fuel servo input to determine the transient response of the system. The procedure was first to set a particular

altitude. Once the altitude was set, then the step disturbance was introduced. The recorders were turned on just prior to the step and turned off after the control system settled out. With a fixed magnitude of disturbance, a series of such disturbances were introduced with different control settings for each transient.

After determining the response of the system for different control settings, another series of transients were run with fixed control settings and various magnitudes of disturbance. And, finally, the effect of altitude on response was determined by introducing a disturbance of a given size at each of several altitudes.

### Range of Variables

All the data presented herein are for a Mach number of 2.76 and altitudes from 68,000 to 82,000 feet. Engine-inlet temperature was held at approximately 528° F.

## RESULTS AND DISCUSSION

The results of this investigation are discussed in two sections. First, some of the engine characteristics of significance in control systems are discussed. These include steady-state performance, transient performance, frequency response, and ignition characteristics. After the general behaviour of the engine has been established, the performance of one of the control systems for the engine is discussed. The data for the one control indicate the general type of performance of all four systems.

### Engine Characteristics

Steady-state performance. - The region in which the engine was operated in steady state is indicated in figure 14. The figure shows the variation of diffuser pressure recovery with actual and ideal (100-percent burner efficiency) fuel-air ratios for several altitudes. For a given recovery, a somewhat greater fuel-air ratio is required as altitude increases.

At high recoveries, slight variations in facility or engine conditions could cause the normal shock within the engine to be expelled, resulting in a breakdown of the supersonic flow to the engine. Since reestablishment of the supersonic flow caused some delay, operation above a pressure recovery of 0.62 was limited. Some data were obtained in this range, however, up to a maximum recovery of approximately 0.63. The curve of ideal fuel-air ratio permits the other data presented herein to be interpreted in terms of different burner configurations.

Transient performance. - A typical response of the engine to a step increase in fuel flow is shown in figure 15. The responses shown are for an initial recovery of 0.5835, a final recovery of 0.6125, and an altitude of 82,000 feet. Since two recorders were used, the variables for the first recorder are shown in figure 15(a) and those for the second recorder in figure 15(b). At the top of each of the figures is a synchronizing trace, which permits the time scales of the two records to be correlated. In addition, the second trace from the top of each record is fuel servo input voltage, which was applied to both records to establish accurately the time at which the disturbance was imposed. All traces shown in figure 15(a) are labeled on the figure.

The traces shown in figure 15(b), from top to bottom, are recorder synchronizing trace, fuel servo input voltage, and eight diffuser innerbody static pressures ( $p_{11}$  to  $p_4$ ). These taps were spaced along the innerbody, as shown in figure 1(b),  $p_{11}$  being near the exit of the diffuser and  $p_4$  being forward in the diffuser near the throat. All the traces move upward for an increase in the variables, and the vertical lines are 0.01 second apart.

After the step increase in fuel servo input voltage was introduced (point A), a little less than 0.01 second elapsed before the fuel flow responded (point B). With the length of tubing and manifold required in the installation of the fuel system, this was about as fast a response as could be obtained. After the fuel flow started to change, it took about another 0.01 second for the fuel-flow response to first reach the final value (point C).

The pressure responses to the fuel-flow disturbance fall into three categories, depending on the location of the normal shock with respect to the particular pressure tap. The three categories consist of (1) those taps which remain in the subsonic region behind the normal shock throughout the transient, (2) those taps which are passed by the normal shock during the transient, and (3) those taps which remain in the supersonic region ahead of the normal shock throughout the transient.

In figure 15(a) all the pressure responses fall into the first category (taps always subsonic). In figure 15(b),  $p_{11}$  to  $p_9$  fall into the first category,  $p_8$  to  $p_5$  fall into the second category (taps passed by normal shock), and  $p_4$  is a borderline case between the second and third categories.

The normal-shock location at the beginning of the transient is between taps 8 and 9, as indicated by the difference in noise level at the beginning of these traces. At the end of the transient, the normal shock has just begun to affect  $p_4$ , as indicated by the pressure fluctuations at points H to J.

The first portion of each pressure response consists of a small interval of dead time during which no change occurs. For example, burner-exit total pressure  $P_{16}$  responds at point D, giving a dead time to fuel flow of approximately 0.012 second. In figure 15(b),  $p_9$ , for example, responds at point E, giving a dead time to fuel flow of 0.031 second.

In the second category,  $p_8$  and  $p_5$  respond at points F and G, respectively. The time interval from the fuel-flow change to these points is not the dead time which is significant in stability studies of control systems, however, but is a longer period of time. This longer period of time is composed of the time from the fuel disturbance until the shock starts to move from its steady-state position plus the time for the normal shock to move from its initial position to the tap of interest. This shock travel time is longer than the time required for a pressure wave to travel the same distance against subsonic flow.

Although this shock passage time is not of primary significance in stability studies of control systems, it is very significant in another respect. For example, if a disturbance occurred either internal or external to the engine, the speed at which the shock moves from its steady-state location to the cowl lip will determine to a large extent how fast the control must be to prevent subcritical operation. Since the shock is moving upstream in this case, and since the air in the forward portion of the diffuser is moving downstream at a high (supersonic) Mach number, a relatively long time is required for the shock to move a given distance. The trace of  $p_5$  in figure 15(b) shows over 0.1 second for the shock to pass that tap (point G). In view of this, an inlet with a slowly varying area near the cowl lip would be advantageous. With such a design, a control could hold the normal shock some distance downstream of the cowl lip with only a relatively small loss in pressure recovery. The longer distance between the steady-state position of the normal shock and the cowl lip would then provide additional time for the control to respond.

An inlet with internal contraction inherently provides some additional length as a result of the diffuser section between the cowl lip and the throat. Diffusers with slowly varying areas near the inlet have been recommended for other reasons. Reference 10 indicates the desirability of a long-throated diffuser for improving diffuser stability.

The third category includes those taps which remain in the supersonic region throughout the transient. The pressures for such tap locations would show no change during the transient. As mentioned previously,  $p_4$ , being a borderline case, shows some fluctuations.

After the initial dead time, the type of response that occurred for those taps in the subsonic region was of either a lag or lead-lag form. In figure 15(a) the response of burner-exit total pressure  $P_{16}$  to fuel flow, for example, is a lag type. Most of the other response traces for pressure taps in the subsonic region are of the lead-lag type. A good example of this latter type of response is  $p_9$  (fig. 15(b)).

The pressure responses for taps which are passed by the normal shock during the transient are of a different nature. After the initial interval in which no response occurs, the type of response varies considerably (see traces  $p_8$  to  $p_5$ ).

The shape of the initial portion of the response is affected by the profile of the normal shock as it passes the given tap and by the speed at which the shock moves past a given tap. The combination of these two things will determine the steepness of the first part of the response. The profile across the normal shock as seen by a tap on the surface of the innerbody is for the most part a boundary-layer shock interaction effect. Once the shock has passed the tap, then the remainder of the response is similar to the last portion of the responses for subsonic taps since now these taps ( $p_8$  to  $p_5$ ) are also subsonic.

Pressure responses for a step decrease in fuel flow with an initial recovery of 0.6125 and a final recovery of 0.5835 are shown in figure 16. The same variables as were presented in figure 15 are shown in this figure. These figures were chosen because they are the smallest steps available in the high-recovery range with a good signal-to-noise ratio.

For a step decrease in fuel flow, the responses again fall into the three categories: pressure tap always subsonic, pressure tap passed by normal shock, and pressure tap always supersonic.

A comparison of the traces ( $P_{16}$  to  $p_9$ ) for taps which are always subsonic shows that the responses for step increases and decreases are very similar. Other pressure responses ( $p_8$  to  $p_4$ ), however, are considerably different for step decreases than for step increases. First, the initial portion of time that elapses before these pressures ( $p_8$  to  $p_4$ ) respond to the fuel-flow change is a shorter dead time, because these taps are in the subsonic region at the beginning of the transient. Next, the shape of the pressure responses after this dead time is different for each tap location and is different than it was for the step increase. Again, the shape of the response is determined by the shock profile and speed as it passes these taps. In this case, however, the shock starts out near  $p_4$  and settles out between  $p_8$  and  $p_9$ ; whereas, for the step increase, it moves in the reverse direction. After the step decrease, the shock slows down as it approaches its final position. As a

result, the response of  $p_8$ , for example, is more gradual than it is for the step increase. For the step decrease,  $p_8$  is near the final position of the shock, and for the step increase it is near the initial position. Since the combination of shock profile and speed varies from tap to tap, and with the direction of the step, the responses for taps which are crossed by the shock vary considerably.

The dead times from a series of transients such as shown in figures 15 and 16 were read and plotted as a function of distance in figure 17. The solid data points are for a step increase. These data tend to fall below the other data points, which are all for step decreases in fuel flow. The dead time varies from approximately 0.018 second for burner-exit static pressure  $p_{13}$  to 0.053 second at  $p_5$ . The data include several step sizes at two different altitudes and are for static pressures only. Note that the initial conditions are different for the step increase than for any of the step decreases. This difference in initial conditions may account for part of the difference between the dead time for the step increase and the dead times for the step decreases. For the step increases most of the data fall within  $\pm 3$  milliseconds of the line faired through the data points. This line curves upward for stations nearer the inlet, indicating that the pressure disturbance travels slower as it moves forward in the diffuser.

The slope of the curve in figure 17 represents the rate of propagation or velocity of the pressure disturbance between diffuser stations. Between the burner inlet and exit, however, the slope does not represent the rate of propagation, since the source of the disturbance is between these stations.

The slope of the curve in figure 17 is presented in figure 18 for the diffuser portion. At the diffuser exit  $p_{12}$ , for example, the rate of propagation is 1180 feet per second. Well forward in the diffuser at the location of one of the control pressure taps  $p_6$ , the rate of propagation is 235 feet per second or approximately one-fifth of that at the diffuser exit. The shape of the curve of figure 18 is related to the air velocities as determined by the diffuser-area variation (fig. 2).

Frequency response. - The results of the frequency-response investigation are shown in figure 19. This figure shows the amplitude ratio as a function of frequency in figure 19(a) and the phase shift against frequency in figure 19(b). Data are presented for burner-exit total pressure  $P_{16}$ , burner-entrance total pressure  $P_{15}$ , and three diffuser static pressures ( $p_{12}$  to  $p_{10}$ ).

The amplitude-ratio - frequency curves for total pressures attenuate similar to a first-order lag. On the other hand, the amplitude-ratio - frequency characteristics for static pressures can be approximated by either a single or several lead-lag functions, depending on the accuracy of approximation desired.

The phase characteristics show the large amount of phase shift, which is typical of dead time. In addition, for the static pressures, the frequency for  $180^\circ$  phase shift (which is significant to control operation) is nearly the same as would be obtained by a calculation of this frequency for values of dead time shown in figure 17.

Ignition characteristics. - During the course of the dynamics investigation, it was found that upon ignition the response of engine pressures was considerably different than that obtained to fuel-flow disturbances after the engine was ignited. During all ignition transients the normal shock would overshoot its final position. A typical ignition transient is shown in figure 20. The propagation of the pressure disturbance upstream from the burner can be traced by noting the time at which each pressure starts to change (points A, B, C, etc.). In figure 20(b), a dashed line has been sketched to indicate the approximate path of the shock during the transient. It is interesting to note that  $p_2$  is affected by the shock and that the shock finally settles out somewhere between taps 4 and 5. This indicates that the amount of overshoot for the shock was approximately 3 feet. This ignition transient was for a fuel-air ratio of 0.0515, which was approximately the richest fuel-air ratio at which ignition was possible without expelling the normal shock from the diffuser during the transient.

A series of ignition transients were run at other fuel-air ratios. The results of these transients are shown in figure 21. This figure shows the variation of diffuser pressure recovery with fuel-air ratio for steady-state operation. For fuel-air ratios up to approximately 0.052, the normal shock remained within the diffuser during ignition transients (including the overshoot). For fuel-air ratios between 0.052 and 0.055 the normal shock was expelled from the engine during ignition transients.

Expulsion of the normal shock from the engine diffuser interfered with the supersonic flow from the free-jet nozzle in front of the engine. As a result, the normal shock did not return as would be expected in flight. For fuel-air ratios above 0.055, the normal shock would be expelled from the diffuser even in steady state.

The data shown in figure 21 indicate that, even though the shock overshoots several feet during the ignition transient, successful ignition (without expelling the shock) was possible at fairly rich fuel-air ratios.

#### Control-System Characteristics

Steady-state performance. - Normally, the settings ( $\beta_3$ ,  $\beta_4$  and the carrier amplifier gains, fig. 13) which determine the operating point

were made at static sea-level conditions from calibration information and were not changed during the time the facility and engine were started and operated.

Once the engine was switched over to automatic control, the system was then operated over a range of altitudes to determine whether the control was operating satisfactorily in steady state. The type of performance attained is illustrated in figure 22, where the control operating line is superimposed on the engine characteristics. The engine characteristics shown are the variation of control pressure for one tap location  $p_{532}$  with diffuser pressure recovery over a range of altitudes.

The control actually is designed to hold a constant ratio of controlled to reference pressure ( $p_{532}/p_{429} = 3.10$ ). Operation at a constant ratio of controlled to reference pressure results in a deviation in total-pressure recovery of approximately 0.003 from a recovery of 0.612. This is approximately a 0.5-percent variation. Since the deviation in pressure recovery is so small, it is difficult to determine whether it is due to imperfect generalization of the control characteristics (fig. 11), whether it is due to small leakages in lines and connections to the pressure sensors, or whether the major portion of the deviation can just be attributed to errors in the measurement of the values of the various pressures in steady state with manometers.

Dynamic performance. - For the first part of the dynamics study, the magnitude of the fuel step disturbance was held constant and different combinations of loop gain and integrator time constant were used for each transient. Response times and the percent overshoot for the transients were then read from the oscillograph records. The response time was defined as the time from the disturbance until the transient first completed 90 percent of its response. This time was measured on the fuel servo input, fuel-valve position, or fuel-flow trace. It was not read on the controlled pressure traces because the relation between the controlled pressures and fuel flow is nonlinear. At low fuel flows (and diffuser pressure recoveries), no change in controlled pressure occurs over a wide range of fuel flows (fig. 11). This "saturation" effect would make the data more difficult to interpret if response time were measured on the controlled pressure trace.

The percent overshoot was measured on the same traces as response time and was defined as the percent of the first overshoot with respect to the disturbance magnitude.

The variation of response time as a function of integrator time constant is shown in figure 23 for several values of loop gain and an altitude of 68,000 feet. Figure 23(a) is for a step increase in fuel flow of 2130 pounds per hour (13.6 percent of fuel flow at max. recovery), and figure 23(b) is for a step decrease in fuel flow of the same

amount for the same controller settings. The data are plotted on semi-log paper to permit easier visualization over a wide range of settings.

The variation of percent overshoot with integrator time constant for the same series of transients (same engine and control conditions) is shown in figure 24(a) for a step increase and in figure 24(b) for a step decrease of the same magnitude (13.6 percent). These figures correspond to figures 23(a) and (b), respectively.

As integrator time constant is decreased (for a constant loop gain), response time decreases and percent overshoot increases. For a given integrator time constant, an increase in loop gain decreases the response time and increases the percent overshoot. These trends are as expected and are typical of all four systems. In addition to these trends, figures 23 and 24 also show the values of loop gain and time constant needed to attain minimum response times with specified mounts of overshoot.

For all the data in figures 23 and 24, the fuel steps were large enough to have placed the engine in the subcritical buzz region without control. However, the control action was fast enough for all control settings investigated to prevent subcritical operation. The magnitude of the step disturbance was 13.6 percent as compared with an increase of 12.3 percent needed to reach critical recovery in steady state.

The minimum response time attained was 0.08 second and the maximum was 0.5 second.

Effect of disturbance magnitude on response. - A pair of values of loop gain and time constant was chosen during the investigation which gave a fast stable response. With the control set at these values (loop gain = 0.710,  $\tau = 0.035$  sec), the system was then subjected to a series of disturbances of different magnitudes. Figure 25 shows that response time varies very little with the magnitude of the disturbance for step sizes from 2130 to 4260 pounds per hour (13.6 to 27.2 percent of fuel flow at **max.** recovery). Furthermore, no subcritical operation occurred during any of the transients even though the magnitude of the disturbance was large enough to place the engine well into the subcritical region in steady state.

Effect of altitude on response. - The effect of altitude on response time is shown in figure 26. The figure indicates that altitude effect is rather small for the step decreases in fuel flow, but that for increasing fuel-flow steps the response time increases as altitude increases.

#### CONCLUDING REMARKS

The results of the investigation of engine dynamics reveal that the predominant dynamic form of the response of engine pressures to fuel flow

is dead time. For static pressures this dead time varied from 0.018 to 0.053 second, depending primarily on the location of the pressure tap. Furthermore, transient and frequency-response data gave nominally the same value for dead time.

Secondary dynamic characteristics (lag or lead-lag) were also consistent for transient and frequency-response data.

It was found that the response of pressures during ignition transients was different than the response obtained to step disturbances in fuel flow after the engine was ignited. Of particular interest is the fact that during all ignition transients the normal shock overshoot its final steady-state position by several feet (3 ft for transient shown).

All four of the control systems investigated were designed to hold a constant ratio of a particular diffuser static pressure to the reference pressure on the inlet-cone surface. Holding that ratio constant resulted in very nearly constant diffuser total-pressure recovery over a range of altitudes. Typical data presented for the  $p_{532}$  control indicated a possible variation in pressure recovery of approximately 0.5 percent.

Data presented for the  $p_{532}$  control also showed that response times as short as 0.08 second were attainable. Furthermore, response time was found to be essentially independent of disturbance size for fuel-flow step sizes from 2130 to 4260 pounds per hour (13.6 to 27.2 percent of fuel flow at max. recovery).

All the fuel step disturbances were large enough to have placed the engine in the subcritical buzz region without control. However, the control response was fast enough for all control settings investigated to prevent subcritical operation. The range of control settings studied gave response times from 0.08 to 0.5 second.

The data for the  $p_{532}$  control is indicative of the performance to be expected from the type of controls investigated.

Lewis Flight Propulsion Laboratory  
National Advisory Committee for Aeronautics  
Cleveland, Ohio, October 17, 1955

## APPENDIX A

## SYMBOLS

$f/a$	fuel-air ratio
$P$	total pressure, lb/sq in.
$p$	static pressure, lb/sq in.
$R$	resistance
$V_e$	error voltage, v
$V_f$	fuel-valve-position feedback voltage, v
$V_i$	fuel servo input voltage, v
$w_a$	air flow, lb/sec
$w_f$	fuel flow, lb/hr
$w_{f,i}$	fuel flow to intermediate spray bars, lb/hr
$w_{f,u}$	fuel flow to upstream spray bars, lb/hr
$\beta$	potentiometer setting (gain)
$\tau$	time constant
Subscripts:	
0	free-stream
1 to 16, 20	location of pressure taps and probes connected to transient instrumentation (figs. 1(b) and 3(b))
12	diffuser exit or burner entrance
13	burner exit
14	diffuser inlet
15	burner inlet
16	burner exit
20	inlet cone

## APPENDIX B

## FUEL SERVO SYSTEM

An electrohydraulic servo system was specially designed to provide the fast response required for ram-jet dynamics and controls investigations. This system controlled the flow to the upstream set of spray bars. The flow to the intermediate set was controlled manually. (The downstream set of spray bars was not used during the controls investigation.)

The electrohydraulic servo system is shown schematically in figure 27. The system positions a fuel metering valve in response to an input voltage signal in the following manner: The input voltage  $V_i$  is compared with a valve-position feedback voltage  $V_f$ , and the difference or error is amplified by a d-c amplifier. The output of the amplifier is fed into a torque motor which moves the pistons of a pilot valve, porting high-pressure hydraulic fluid to the appropriate side of a hydraulic throttle servo. The position of the throttle is sensed by a differential transformer-type position transducer energized by an oscillator. The output signal of the transducer is amplified, demodulated, and filtered, giving the position feedback voltage. The system was designed to give a linear relation between input voltage and throttle position. The principles used in the design of the throttle servo are described in reference 11.

The fuel metering valve incorporates a fast-acting differential relief valve which maintains a constant pressure differential across a metering orifice. Fuel flow, therefore, varies linearly with throttle position. The differential relief valve was designed for fast response and stability according to the method described in reference 12.

## REFERENCES

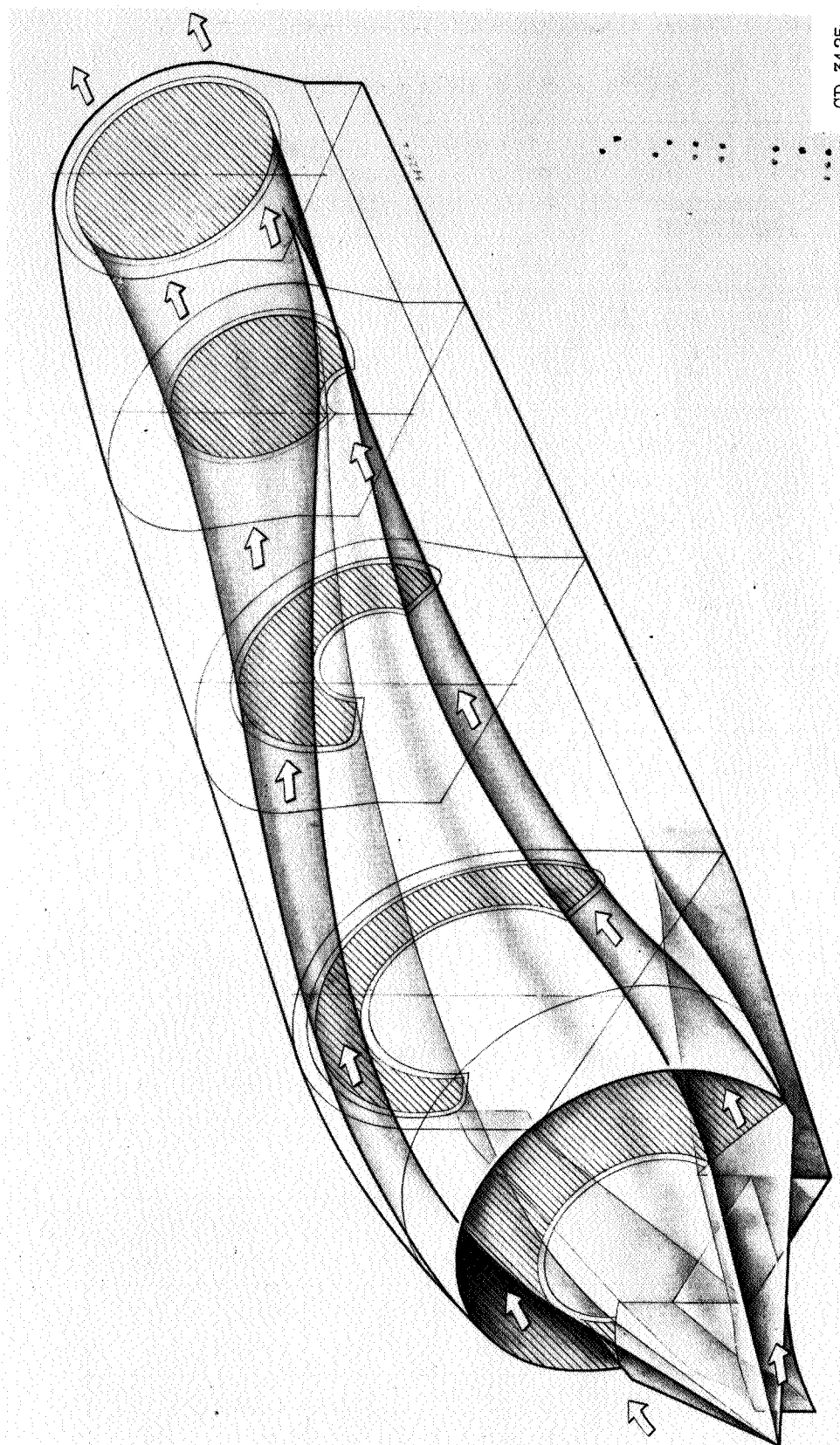
1. Boksenbom, Aaron S., and Novik, David: Control Requirements and Control Parameters for a Ram Jet with Variable-Area Exhaust Nozzle. NACA RM E8H24, 1948.
2. Himmel, Seymour C.: Some Control Considerations for Ram-Jet Engines. NACA RM E52F10, 1952.
3. Vasu, G., Wilcox, F. A., and Himmel, S. C.: Preliminary Report of Experimental Investigation of Ram-Jet Controls and Engine Dynamics. NACA RM E54H10, 1954.

- 3751
4. Hurrell, Herbert G., Vasu, George, and Dunbar, William R.: Experimental Study of Shock-Positioning Method of Ram-Jet Engine Control. NACA RM E55F21, 1955.
  5. Dunbar, William R., Vasu, George, and Hurrell, Herbert G.: Experimental Investigation of Direct Control of Diffuser Pressure on 16-Inch Ram-Jet Engine. NACA RM E55D15, 1955.
  6. Farley, John M., and Seashore, Ferris L.: Full-Scale, Free-Jet Investigation of Methods of Improving Outlet Flow Distribution in a Side-Inlet Supersonic Diffuser. NACA RM E54L31a, 1955.
  7. Meyer, Carl L., and Welna, Henry J.: Investigation of Three Low-Temperature-Ratio Combustor Configurations in a 48-Inch-Diameter Ram-Jet Engine. NACA RM E53K20, 1954.
  8. Rayle, Warren D., Smith, Ivan D., and Wentworth, Carl B.: Preliminary Results from Free-Jet Tests of a 48-Inch-Diameter Ram-Jet Combustor with an Annular-Piloted Baffle-Type Flameholder. NACA RM E54K15, 1955.
  9. Seashore, Ferris L., and Hurrell, Herbert G.: Starting and Performance Characteristics of a Large Asymmetric Supersonic Free-Jet Facility. NACA RM E54A19, 1954.
  10. Kantrowitz, Arthur: The Formation and Stability of Normal Shock Waves in Channel Flows. NACA TN 1225, 1947.
  11. Gold, Harold, Otto, Edward W., and Ransom, Victor L.: Dynamics of Mechanical Feedback-Type Hydraulic Servomotors under Inertia Loads. NACA Rep. 1125, 1953. (Supersedes NACA TN 2767.)
  12. Otto, Edward W., Gold, Harold, and Hiller, Kirby W.: Design and Performance of Throttle-Type Fuel Controls for Engine Dynamics Studies. NACA TN 3445, 1955.
- 1

TABLE I- - PRESSURE-PICKUP INSTALLATION

RECORD FOR 48-INCH RAMJET ENGINE

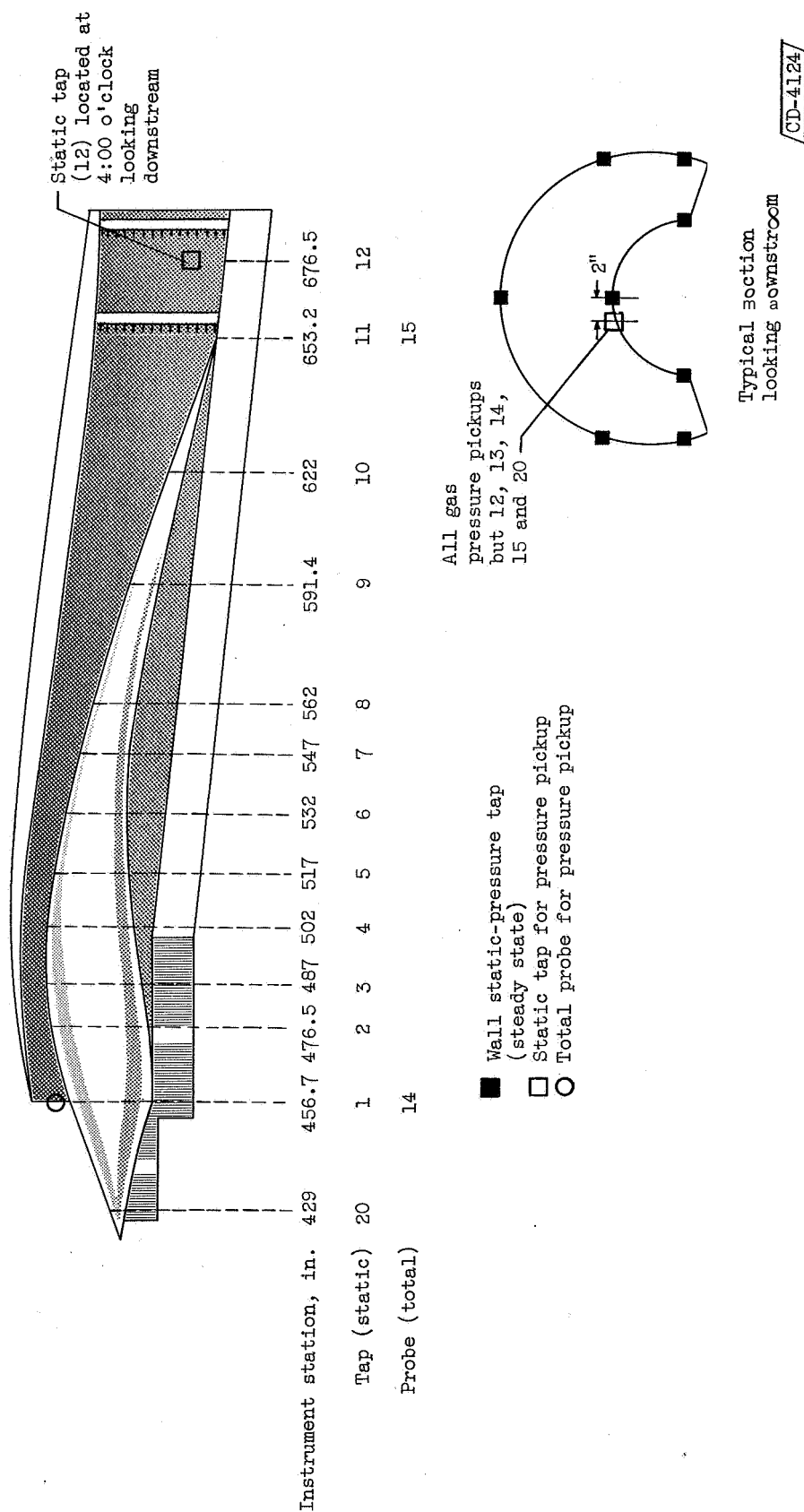
Measured variable	Station, in.	Pickup range, lb/sq in.	Tul ng		Pickup type
			Length in.	I.D., in.	
$p_1$	456.69	0 $\pm$ 15	9	0.040	I
$p_2$	476.50	0 $\pm$ 15	9	0.040	I
$p_3$	487.00	0 k15	9	0.040	I
$p_4$	502.00	0 $\pm$ 15	9	0.040	I
		0 $\pm$ 10	9	.040	II
$p_5$	517.00	0 $\pm$ 15	9	0.040	I
		0 $\pm$ 10	9	.040	III
$p_6$	532.00	0 $\pm$ 15	9	0.040	I
		0 k15	9	.040	II
$p_7$	547.00	0 $\pm$ 15	9	0.040	I
$p_8$	562.00	0 $\pm$ 15	9	0.040	I
$p_9$	591.35	0 $\pm$ 15	9	0.040	I
$p_{10}$	622.00	0 k15	9	0.040	11
		0 $\pm$ 15	9	.040	
$p_{11}$	653.15	0 $\pm$ 15	9	0.040	I
$p_{12}$	676.50	0 $\pm$ 15	9	0.040	I
$p_{13}$	792.00	0 $\pm$ 15	9	0.040	I
$p_{20}$	429.00	0 $\pm$ 15			I
		0 $\pm$ 15			III
$p_{14}$	456.69	0 $\pm$ 15	9	0.040	I
		0 $\pm$ 15	9	.040	III
$p_{15}$	653.15	0 $\pm$ 10	9.5	0.040	III
		0 $\pm$ 15	9.5	.040	I
$p_{16}$	792.00	0 $\pm$ 15	23.75	0.040	II
		0 $\pm$ 15	23.75	.040	I



CD-3425

(a) Isometric view.

Figure 1 - Ram-jet diffuser.



(b) Details of instrumentation.

Figure 1. - Concluded. Ram-jet diffuser.

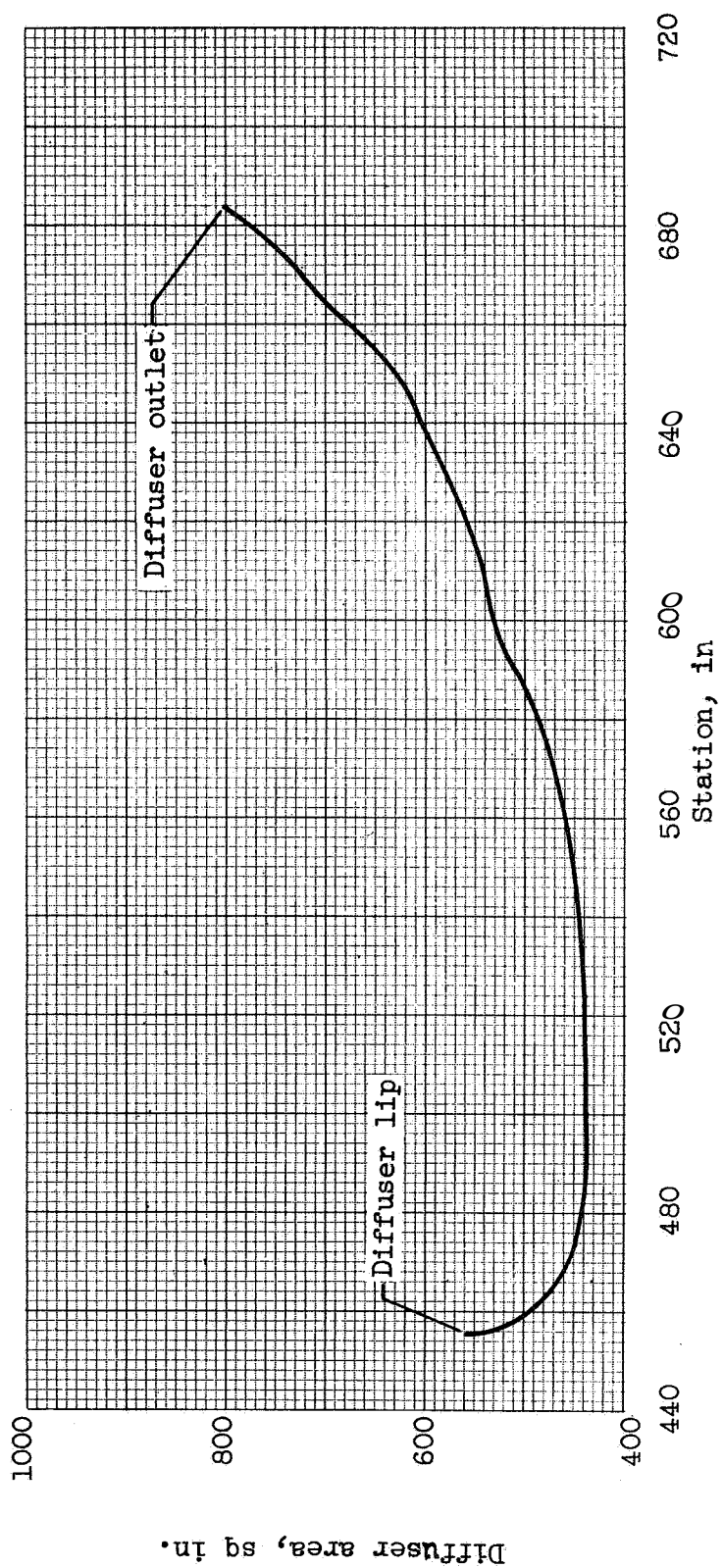
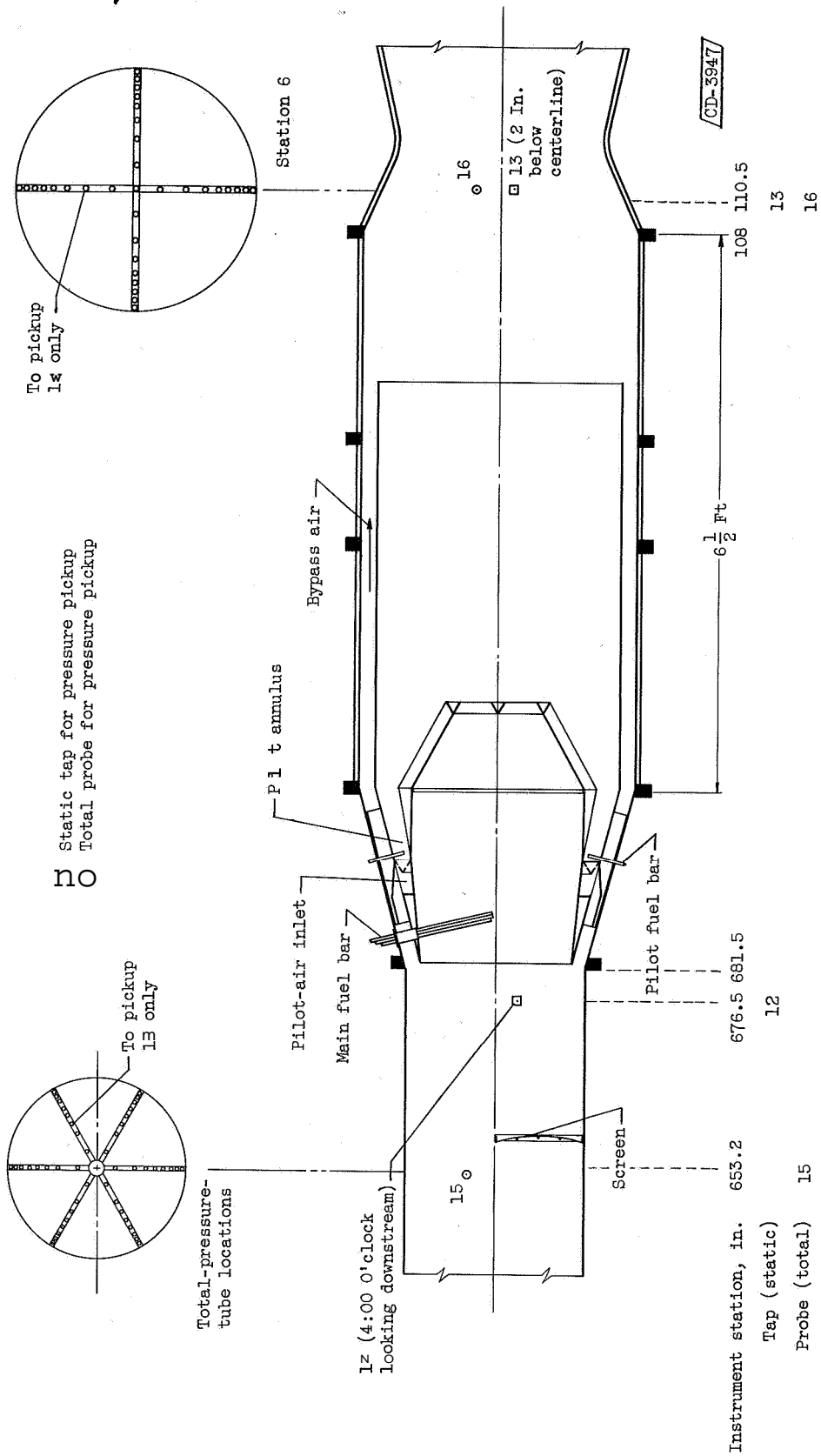
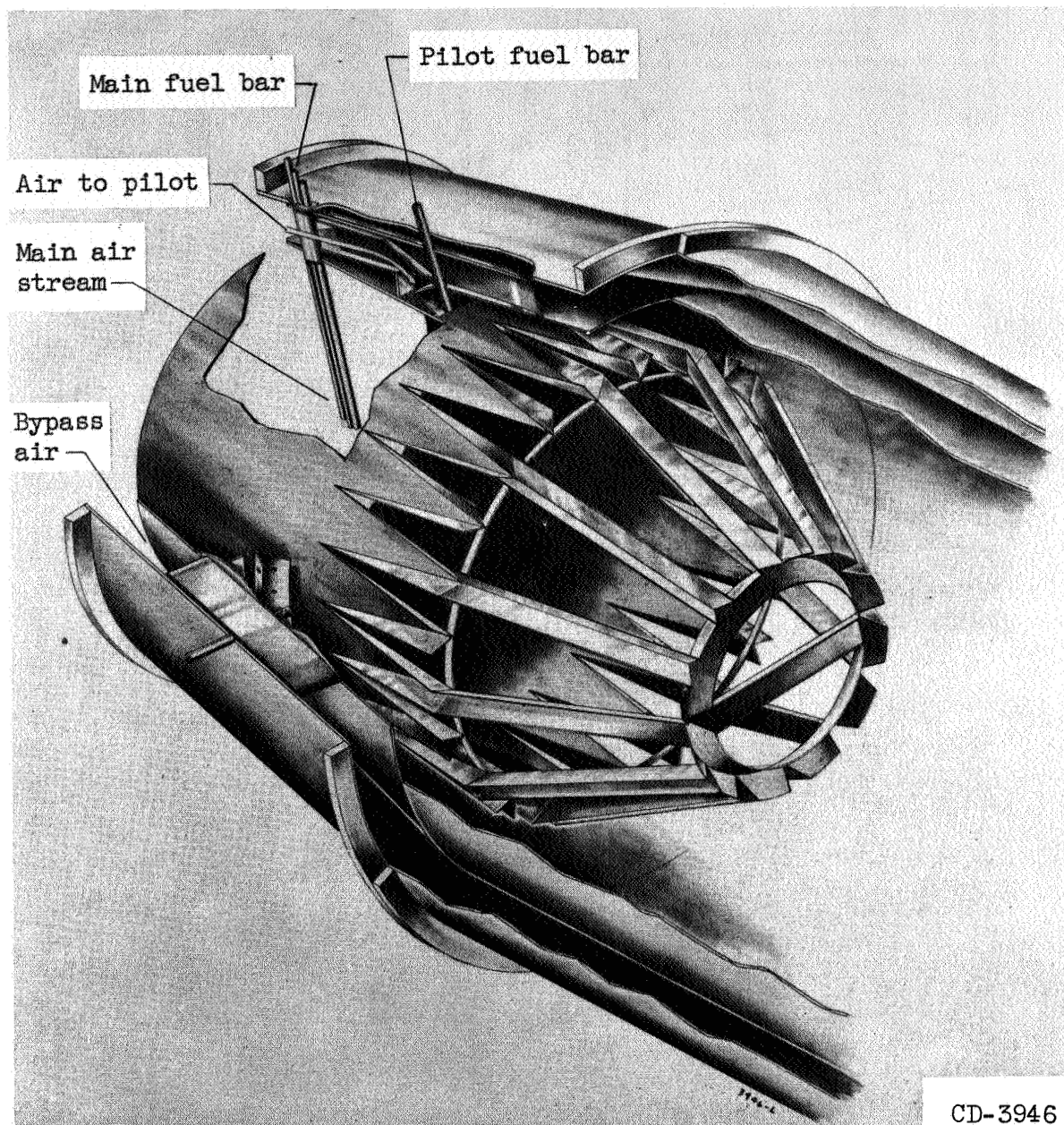


Figure 2. - Diffuser-area variation.



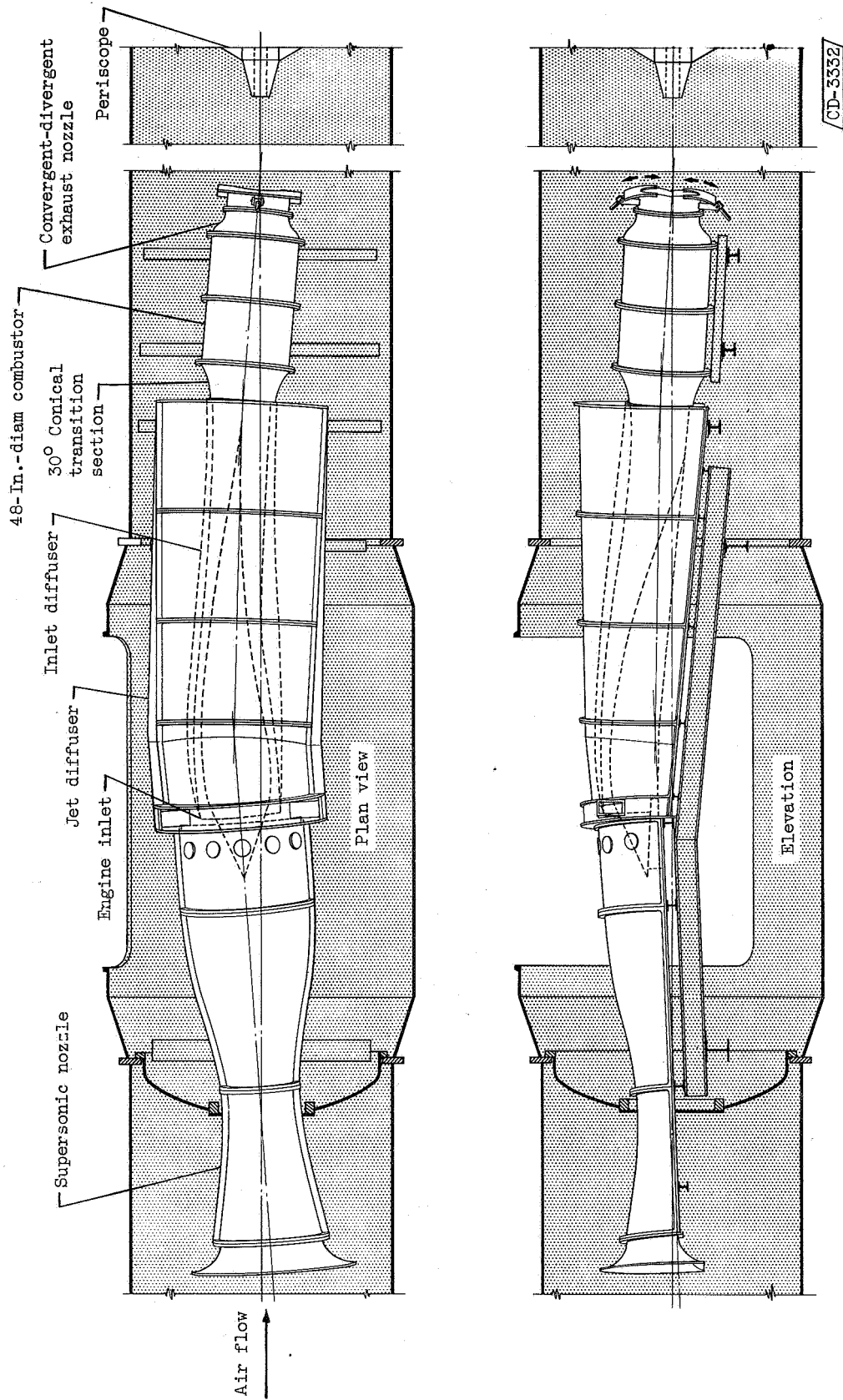
( ) Cross section.

Figure 3. - 48-Inch ram-jet combustor.



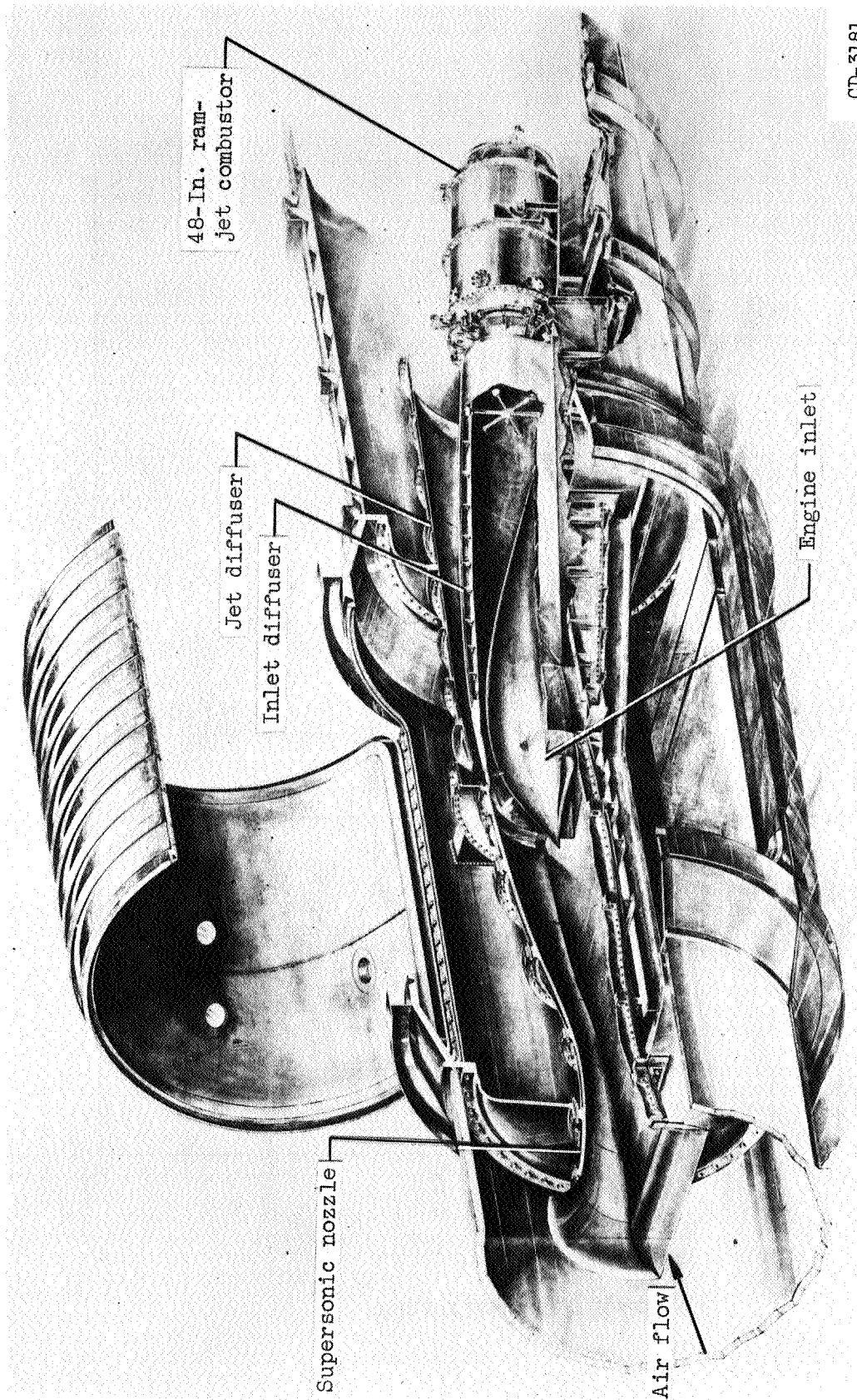
(b) Cutaway view.

Figure 3. - Concluded. 48-Inch ram-jet combustor.



(a) Schematic diagram.

Figure 4. - Free-jet installation of 48-inch ram-jet engine.



CD-3181

(b) Cutaway view.

Figure 4. - Concluded. Free-jet installation of 48-inch ram-jet engine.

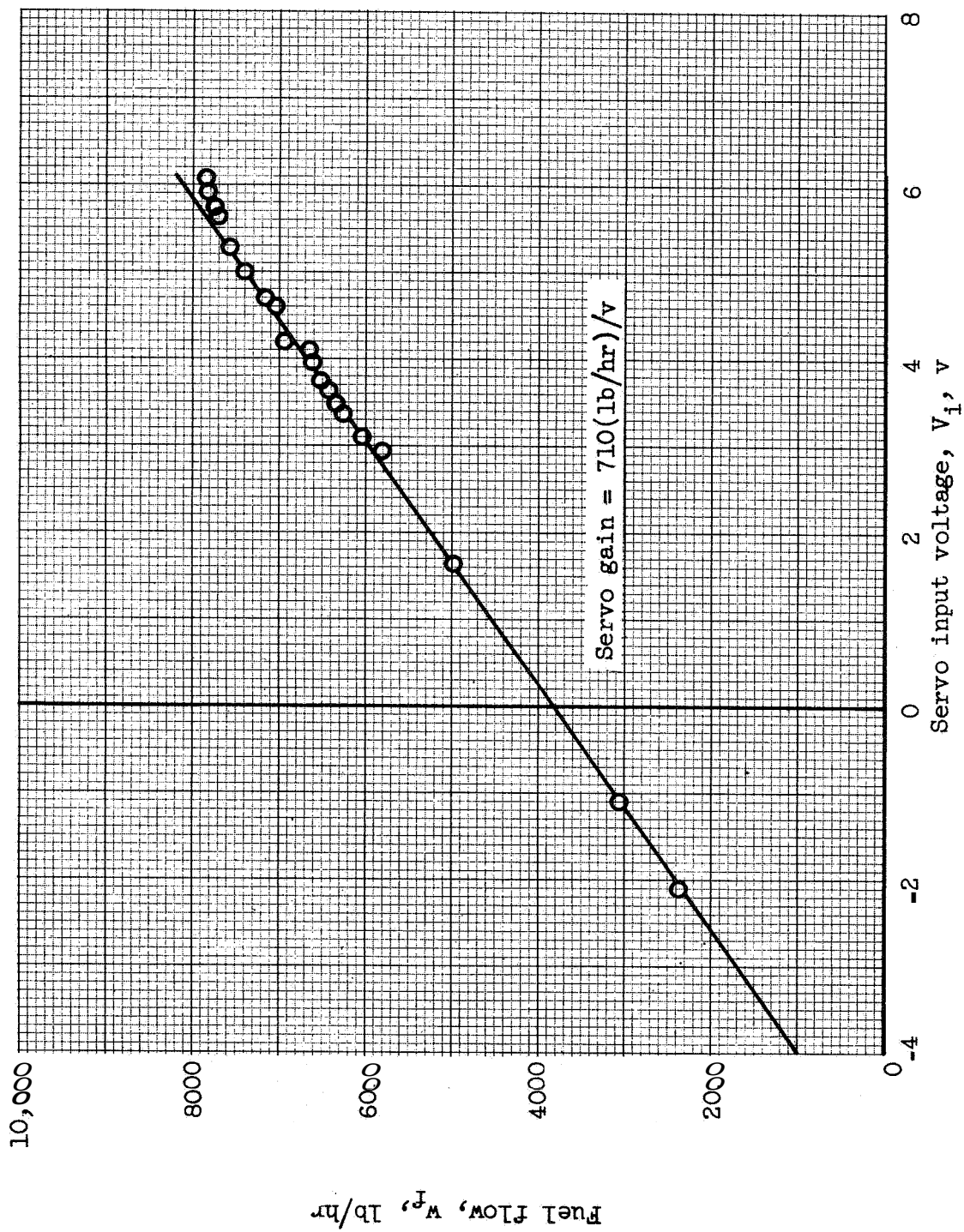
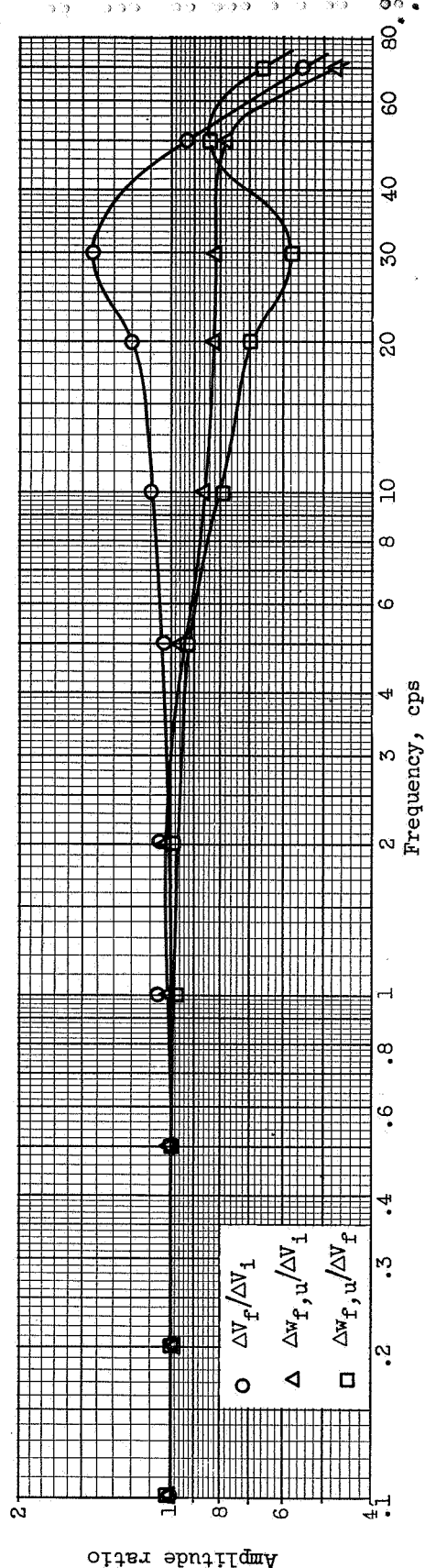
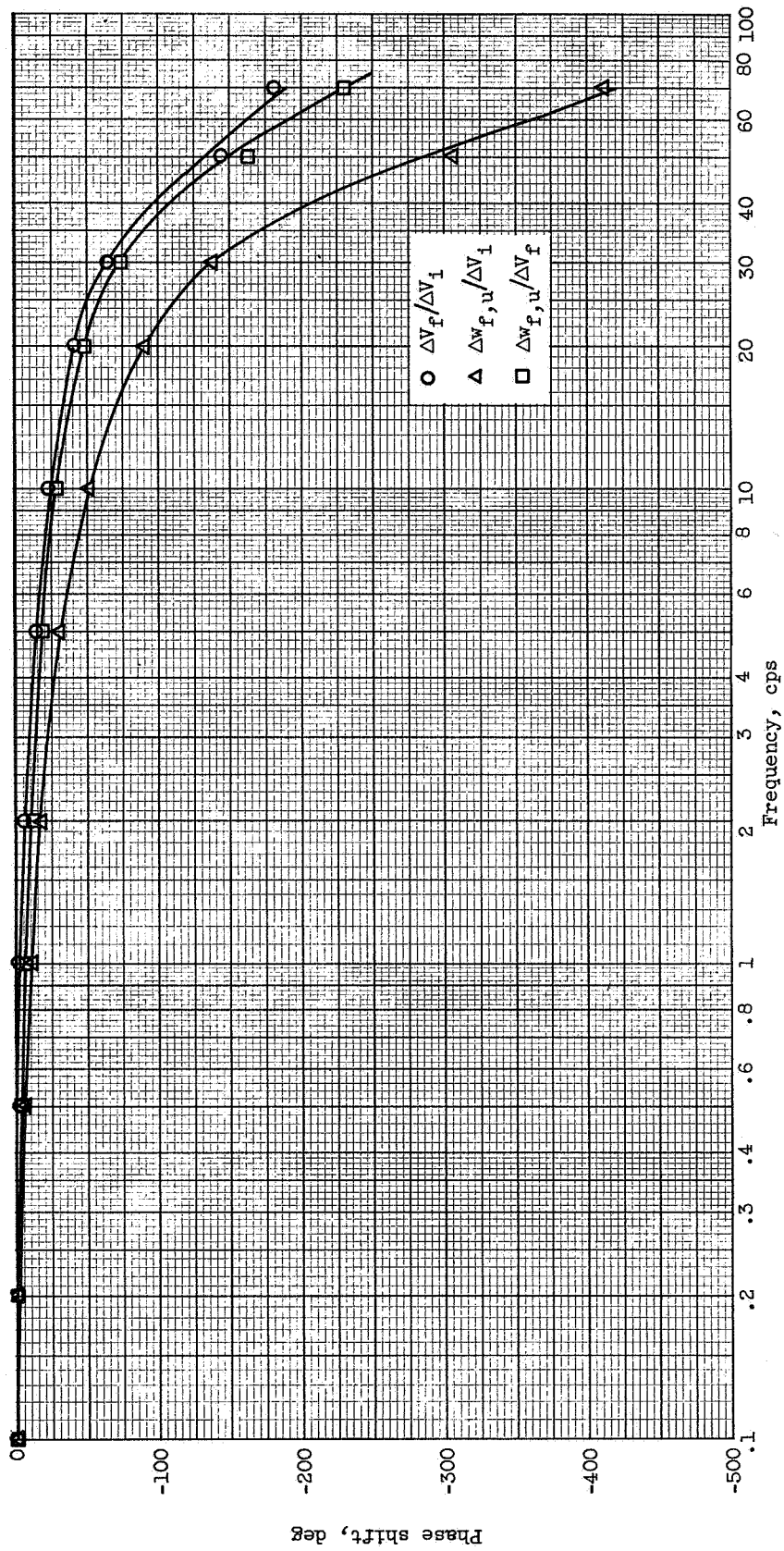


Figure 5. - Calibration of fuel servo system.



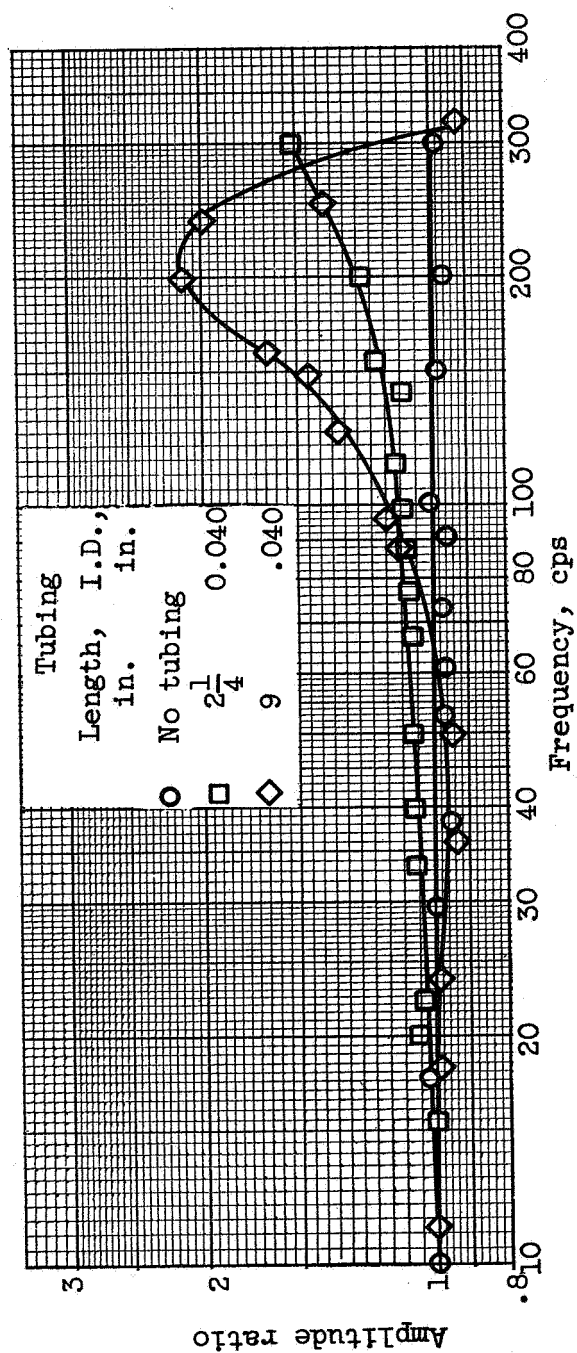
(a) Amplitude ratio.

Figure 6. - Frequency response of fuel system.  $B\omega$  point  $w_{f,u}$ , 6050 pounds per hour; amplitude  $\Delta w_{f,u}$ , 2900 pounds per hour.



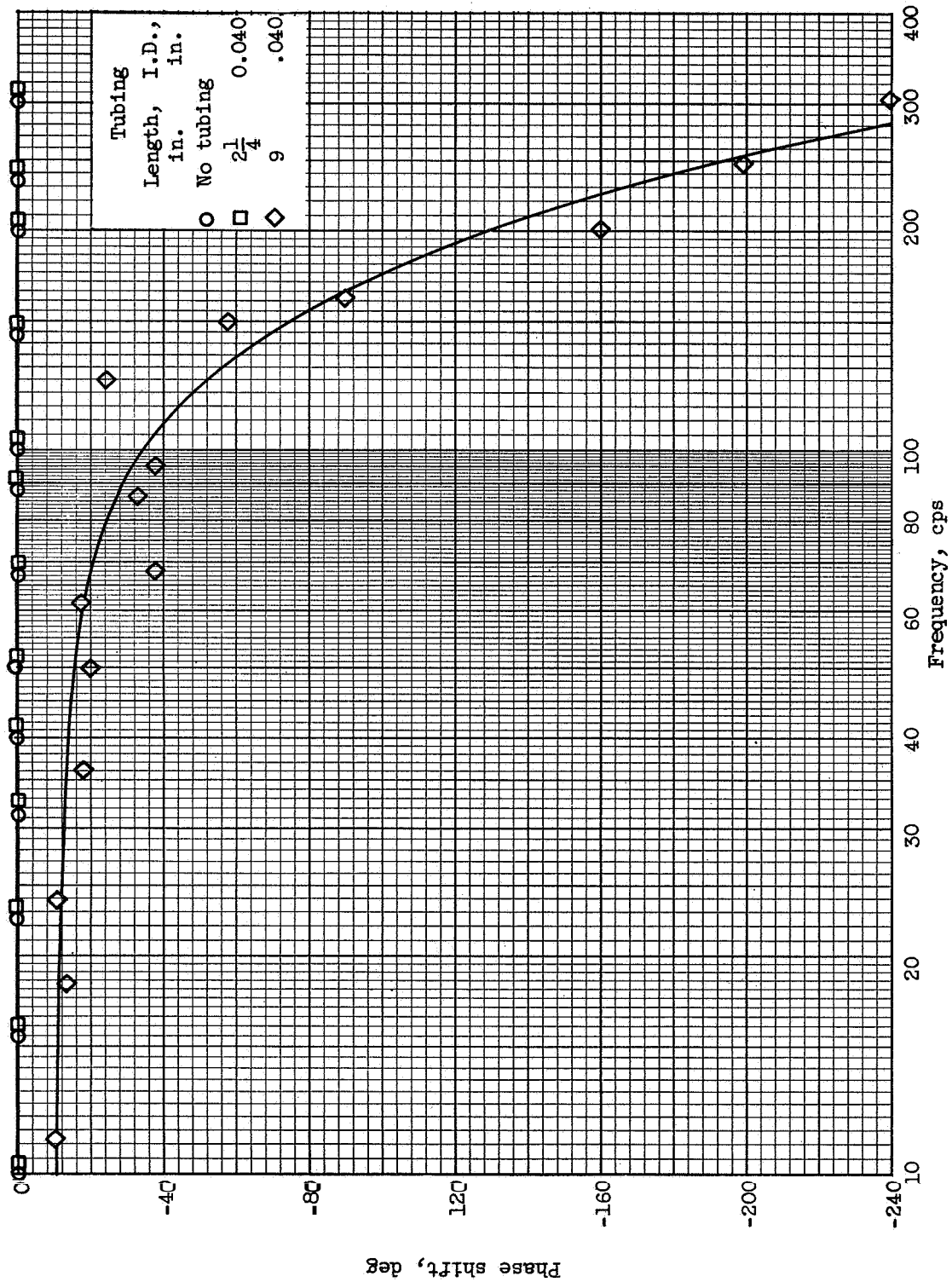
(b) Phase shift.

Figure 6. - Concluded. Frequency response of fuel system. Base point  $w_{f,u}$ , 6050 pounds per hour; amplitude  $\Delta w_{f,u}$ , 2900 pounds per hour.



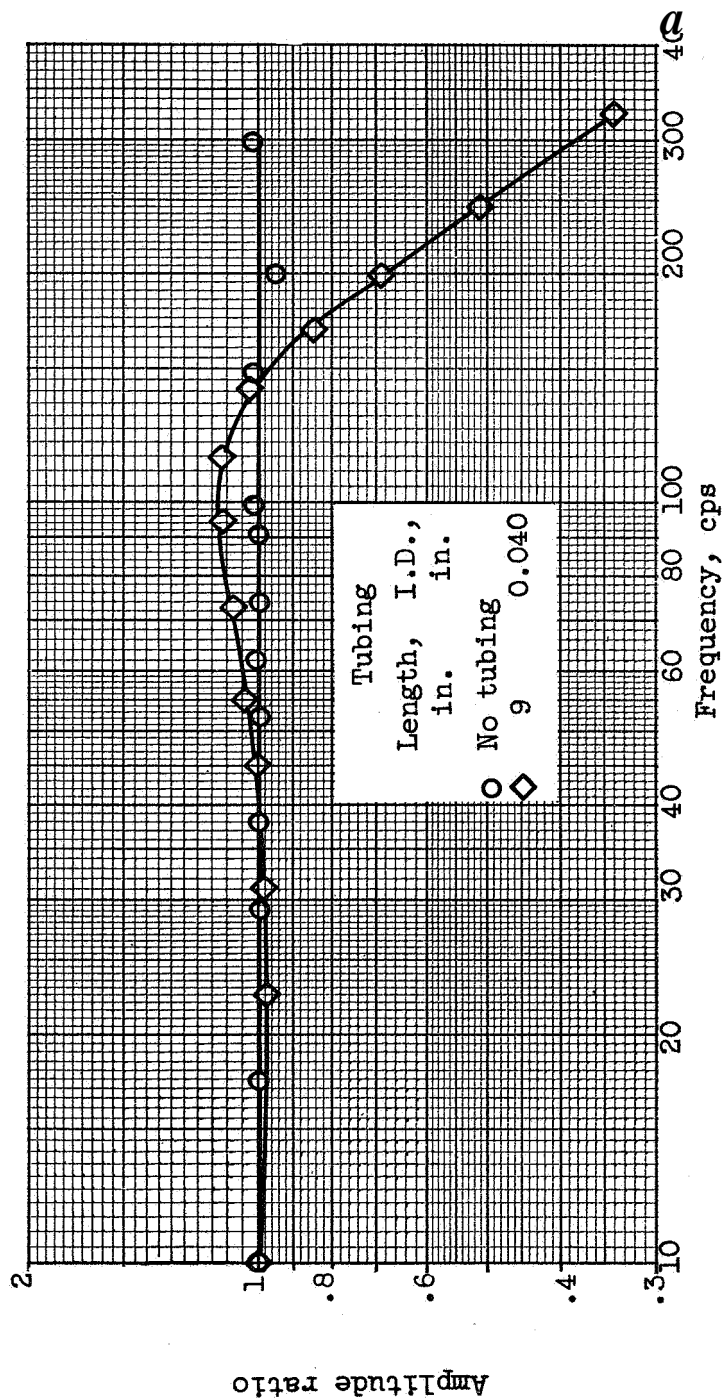
(a) Amplitude ratio.

Figure 7. - Frequency response of type I pressure transducer.



(b) Phase shift.

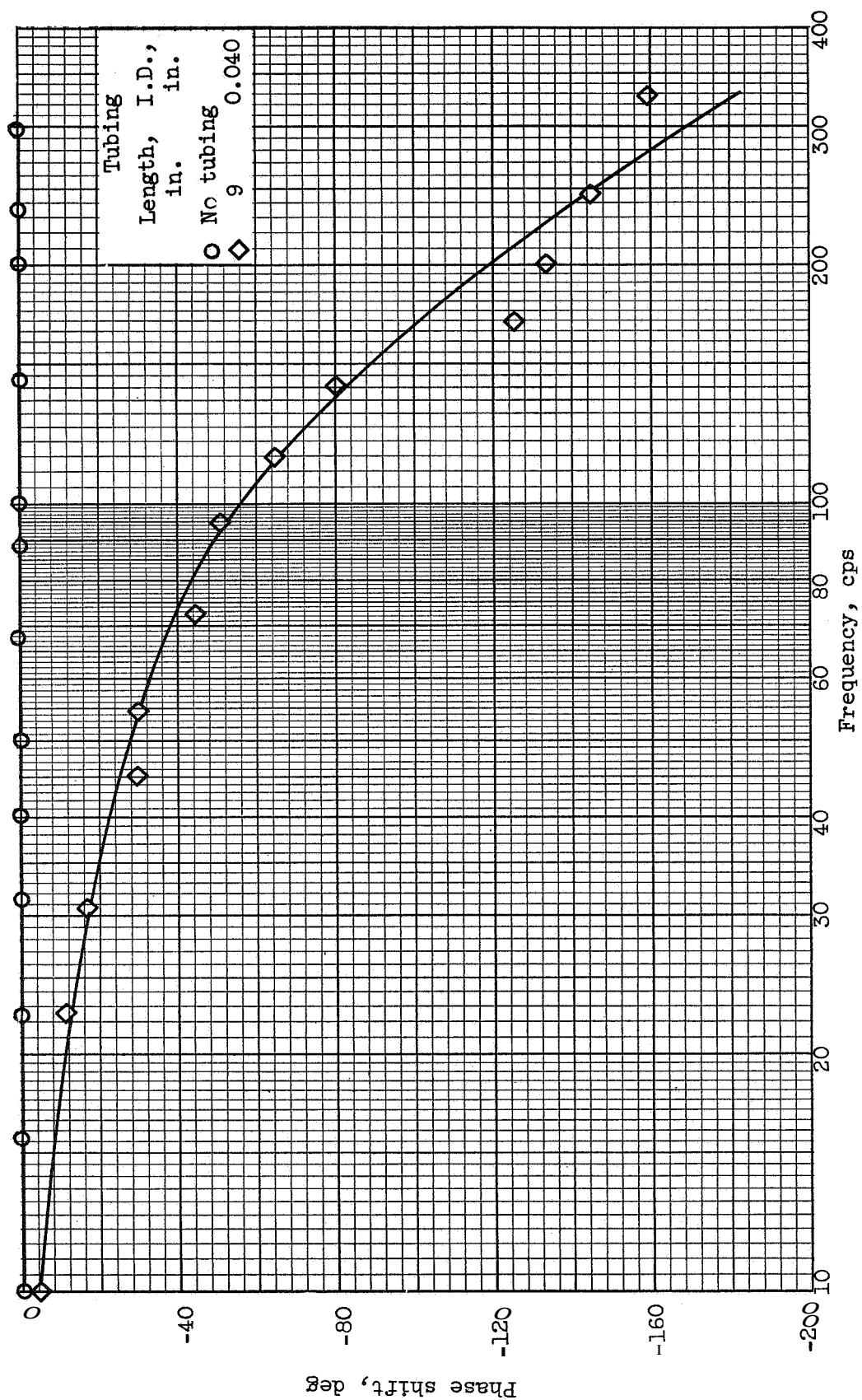
Figure 7 - Concluded. Frequency response of type I pressure transducer.



(a) Amplitude ratio.

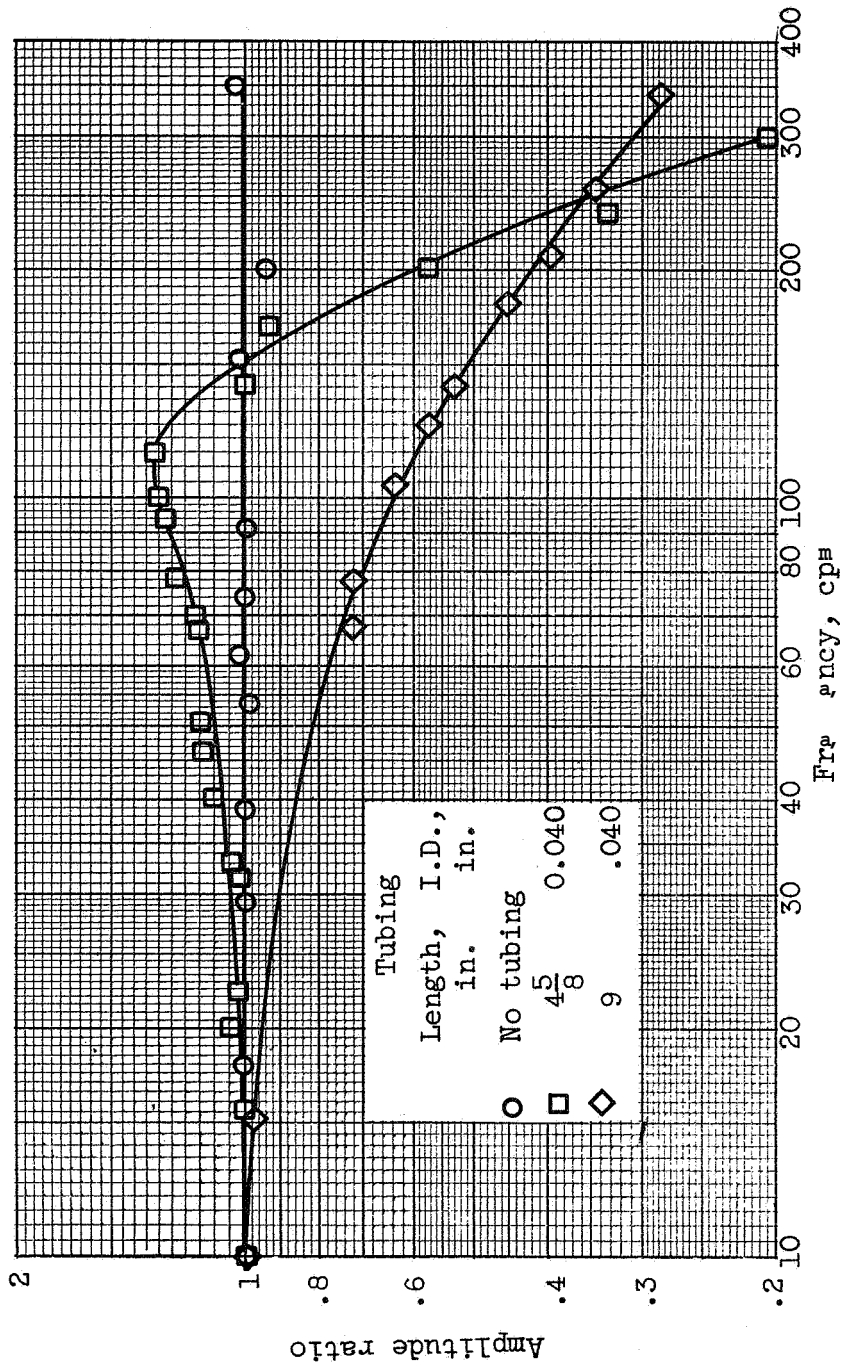
Figure 8. - Frequency response of type II pressure transducer.

CONFIDENTIAL



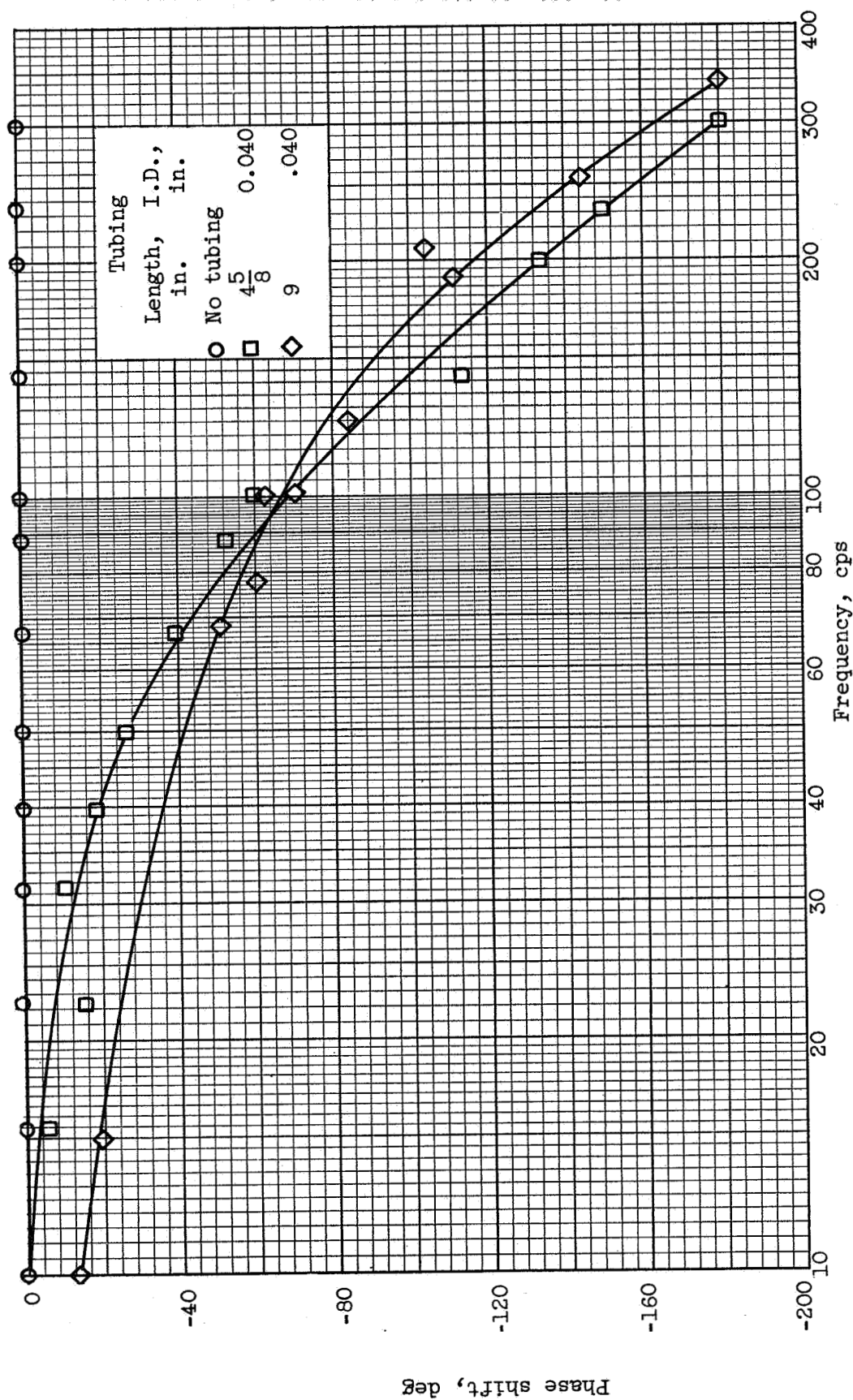
(b) Phase shift.

Figure 8. - Concluded. Frequency response of type II pressure transducer.



(a) Amplitude ratio

Figure 9. - Frequency response of type HII pressure transducer.



(b) Phase shift.

Figure 9. - Concluded. Frequency response of type III pressure transducer.

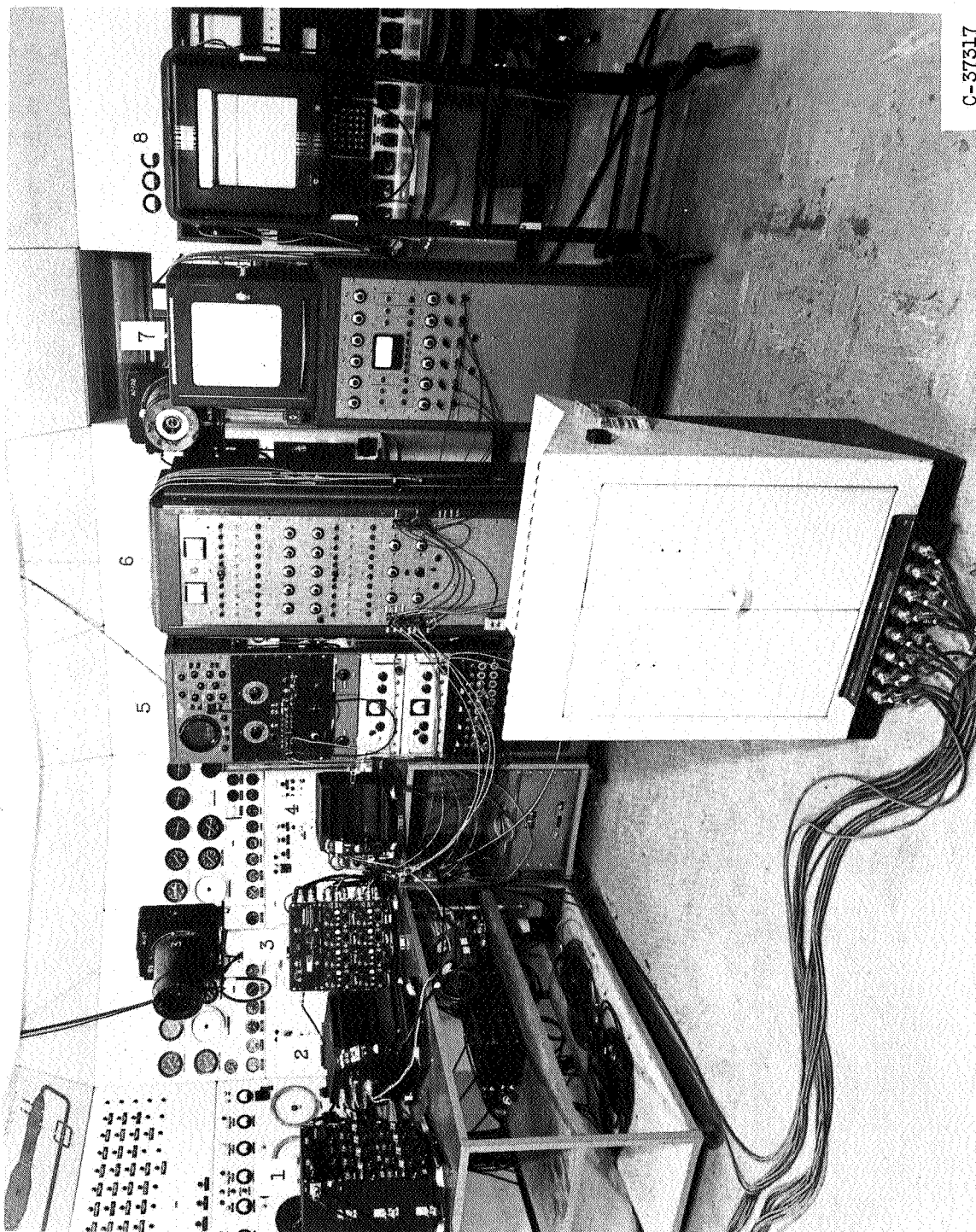


Figure 10 - Computer and recording equipment.

3751

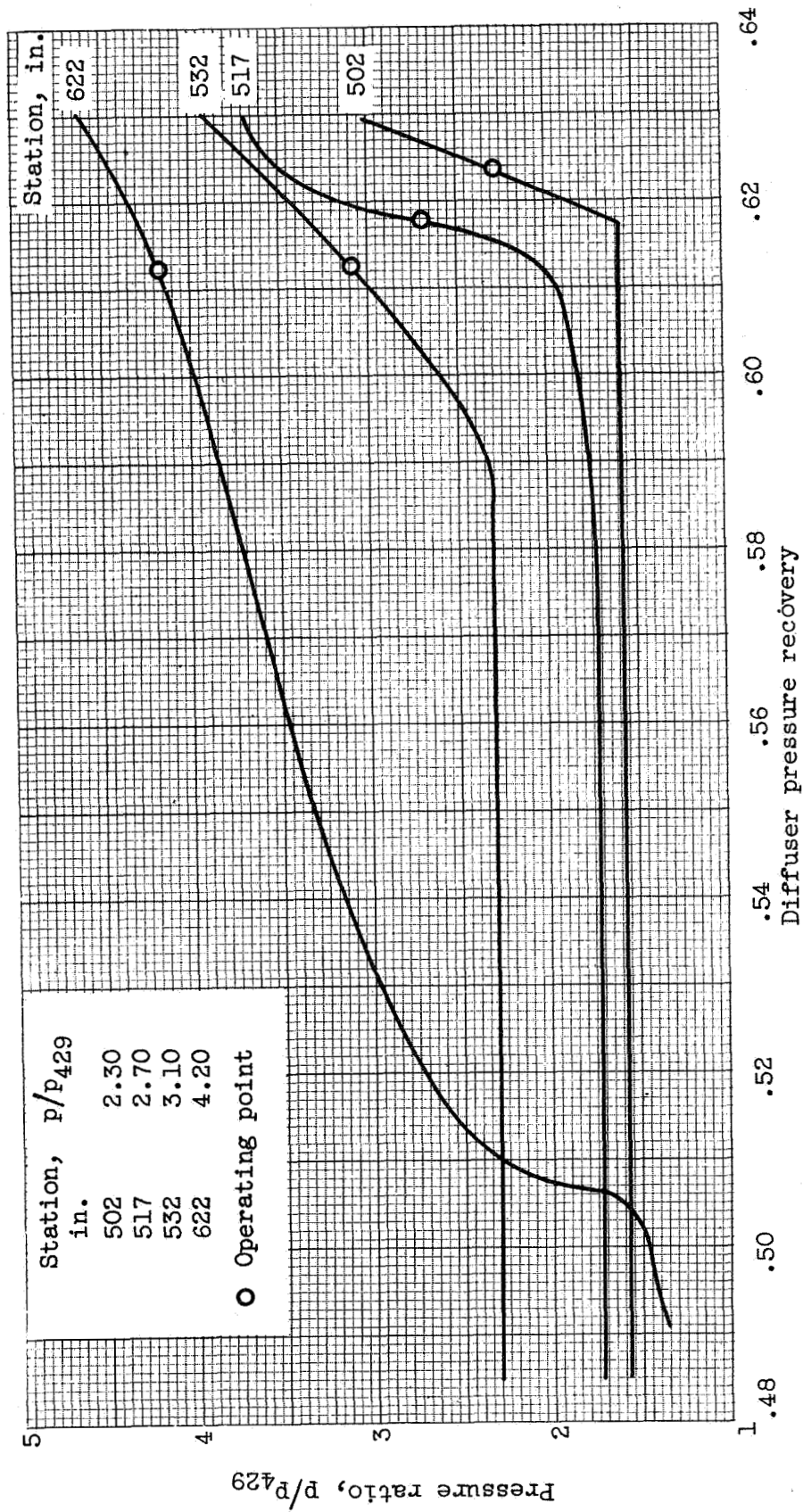


Figure 11. - Ratio of controlled pressure to reference pressure  $p/p_{429}$  for each control stream Mach number, 2.76; engine-inlet temperature, 528° F.

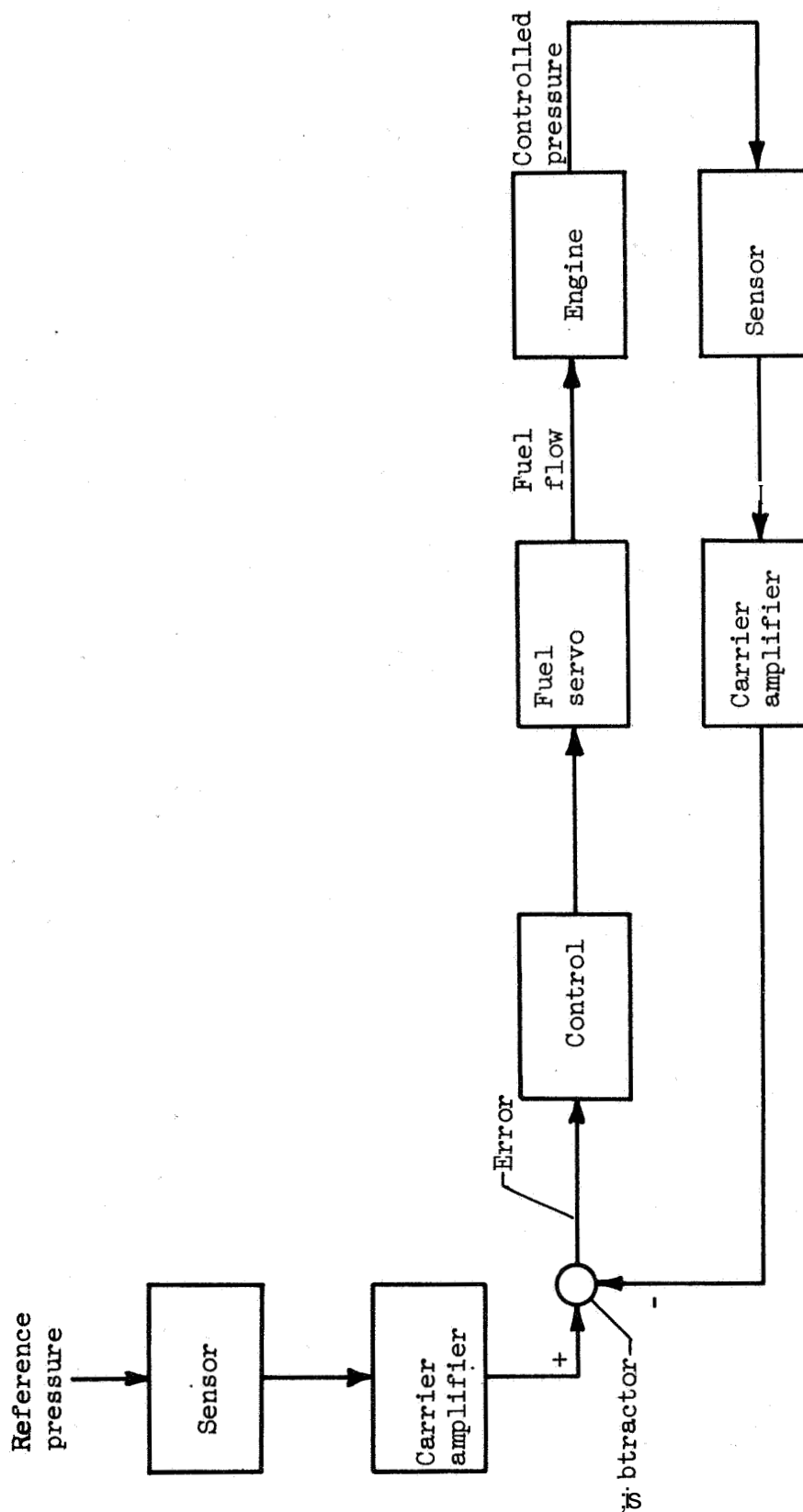


Figure 12. - Block diagram of control system.



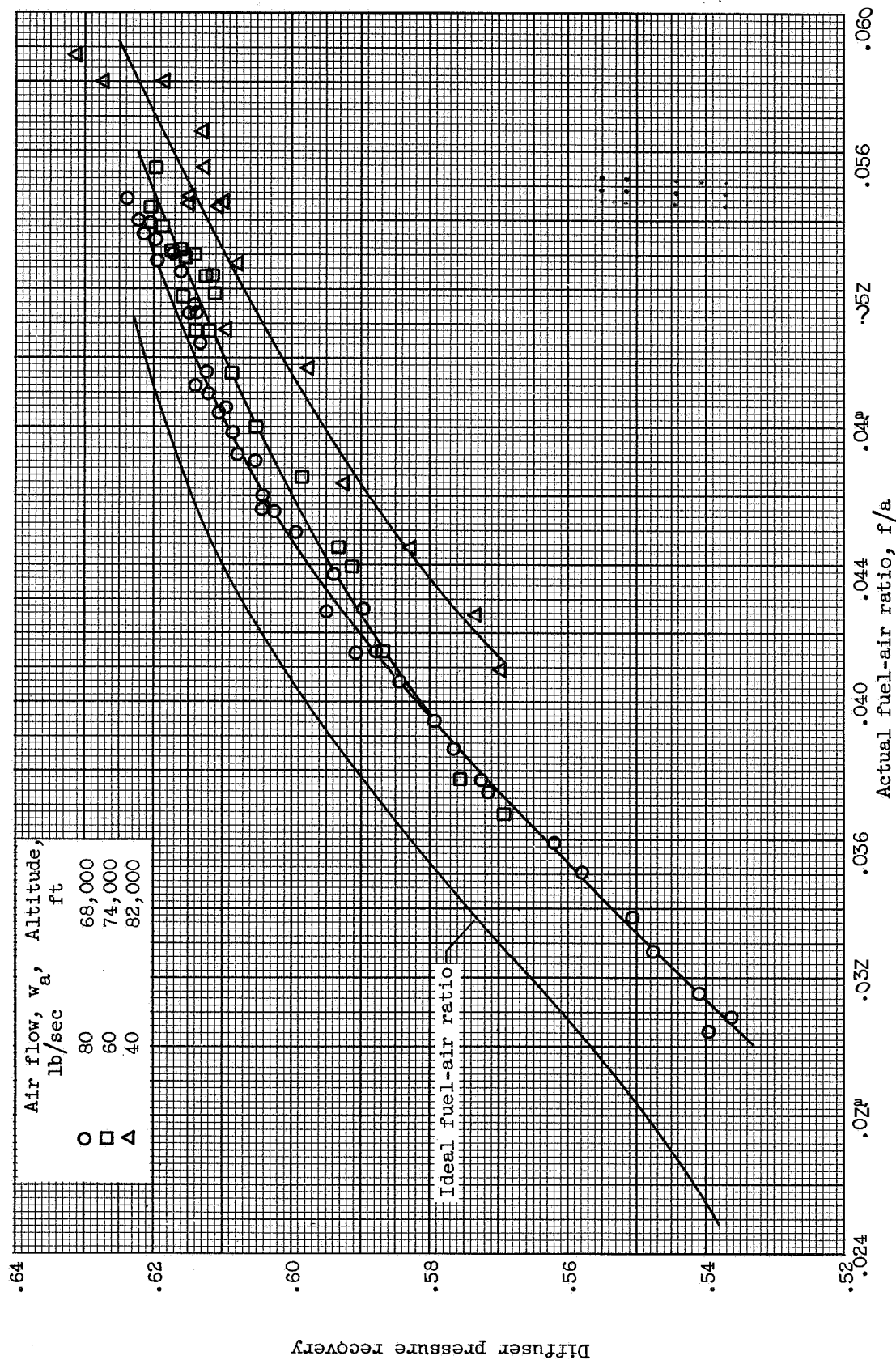


Figure 14. - Variation of diffuser pressure recovery with fuel-air ratio Free-stream Mach number,  $Z 76$ ; engine inlet temperature,  $5280^\circ \text{F}$ .

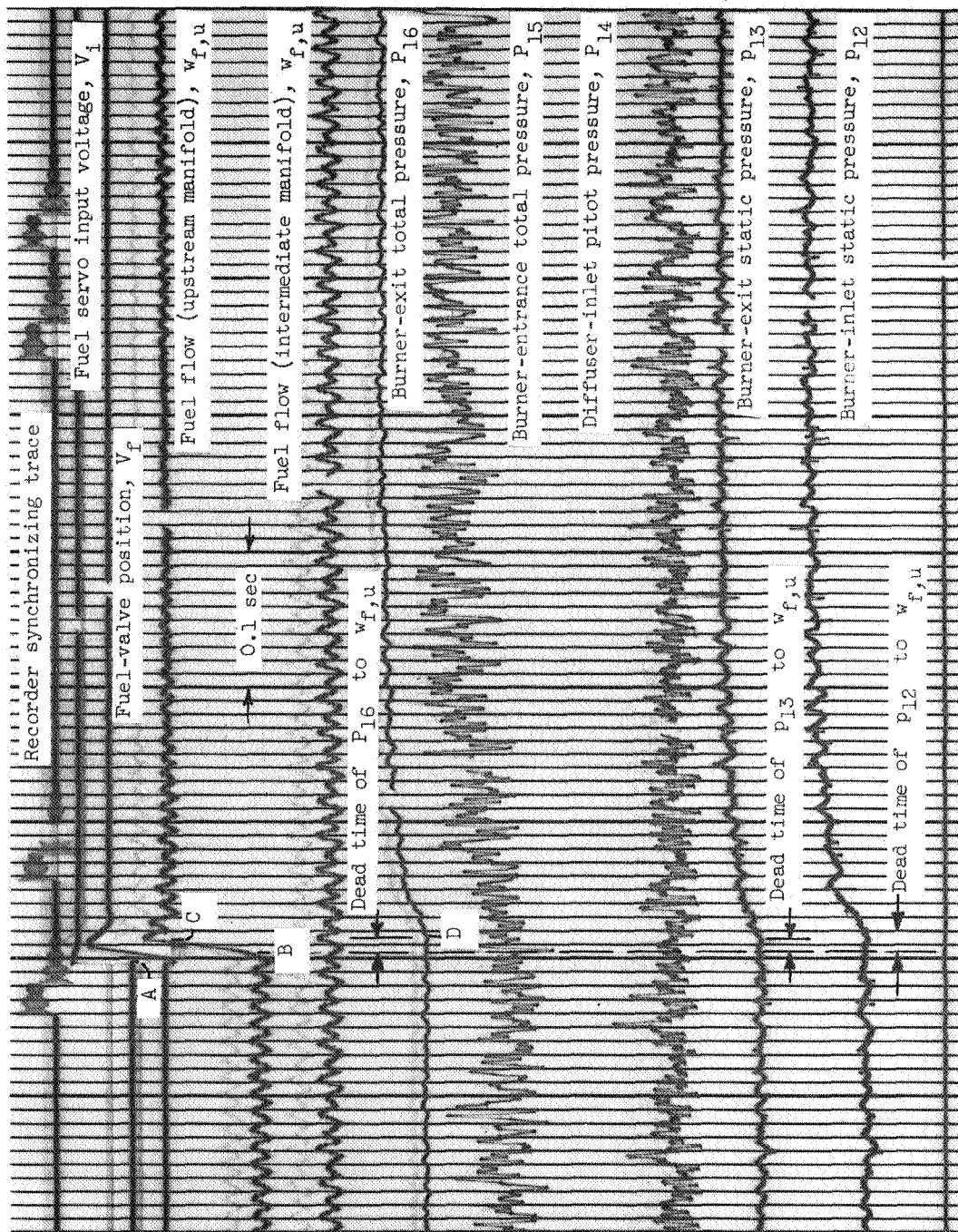
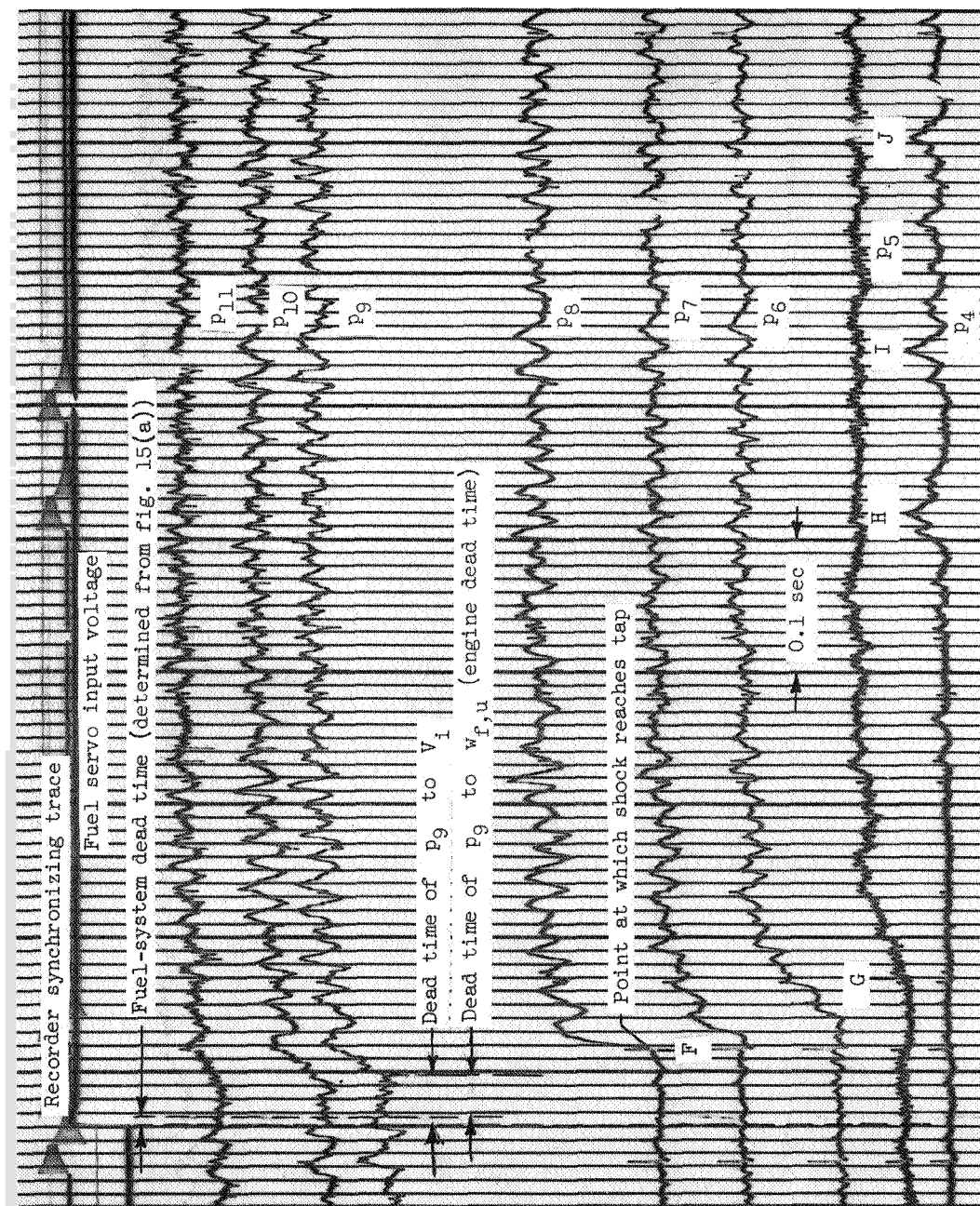
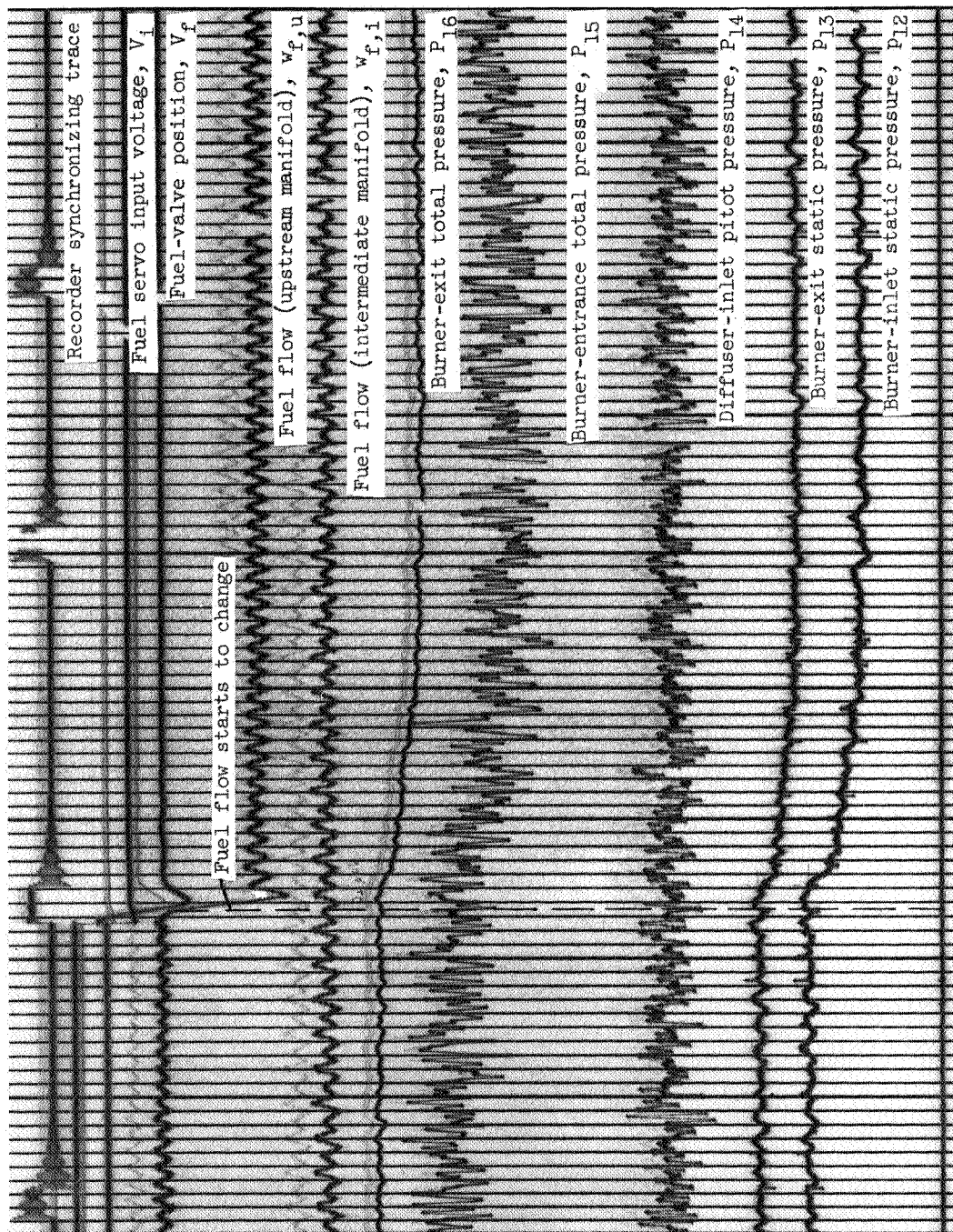


Figure 15. - Response of engine and diffuser pressures to step increase in fuel flow. Altitude, 82,000 feet; initial recovery, 0.5835; final recovery, 0.6125; free-stream Mach number, 2.76; engine-inlet temperature, 528° F.



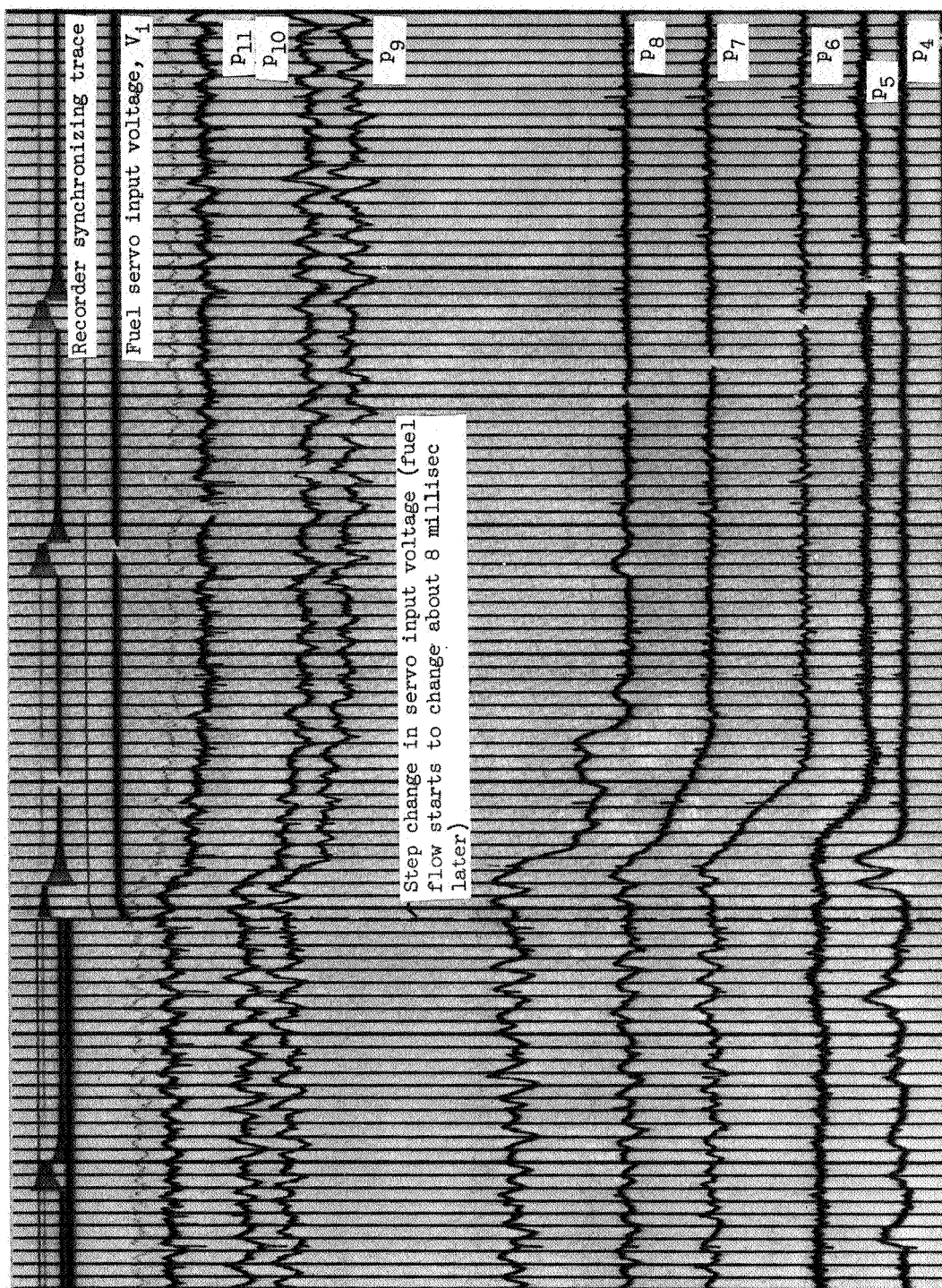
(b) Recorder 2

Figure 15. - Concluded. Response of engine and diffuser pressures to step increase in fuel flow  
 Altitude, 82,000 feet; initial recovery, 0.5835; final recovery, 0.6125; free-stream Mach number, 2.76; engine-inlet temperature, 5280° F



(a) Recorder 1

Figure 16. - Response of engine and diffuser pressures to step decrease in fuel flow. Altitude, 82,000 feet; initial recovery, 0.6125; final recovery, 0.5835; free-stream Mach number, 2.76; engine-inlet temperature, 522° F.



(b) Recorder 2

Figure 16. - Concluded. Response of engine and diffuser pressures to step decrease in fuel flow.  
 Altitude, 82,000 feet; initial recovery, 0.6125; final recovery, 0.5835; free-stream Mach number, 2.76; engine-inlet temperature, 528° F.

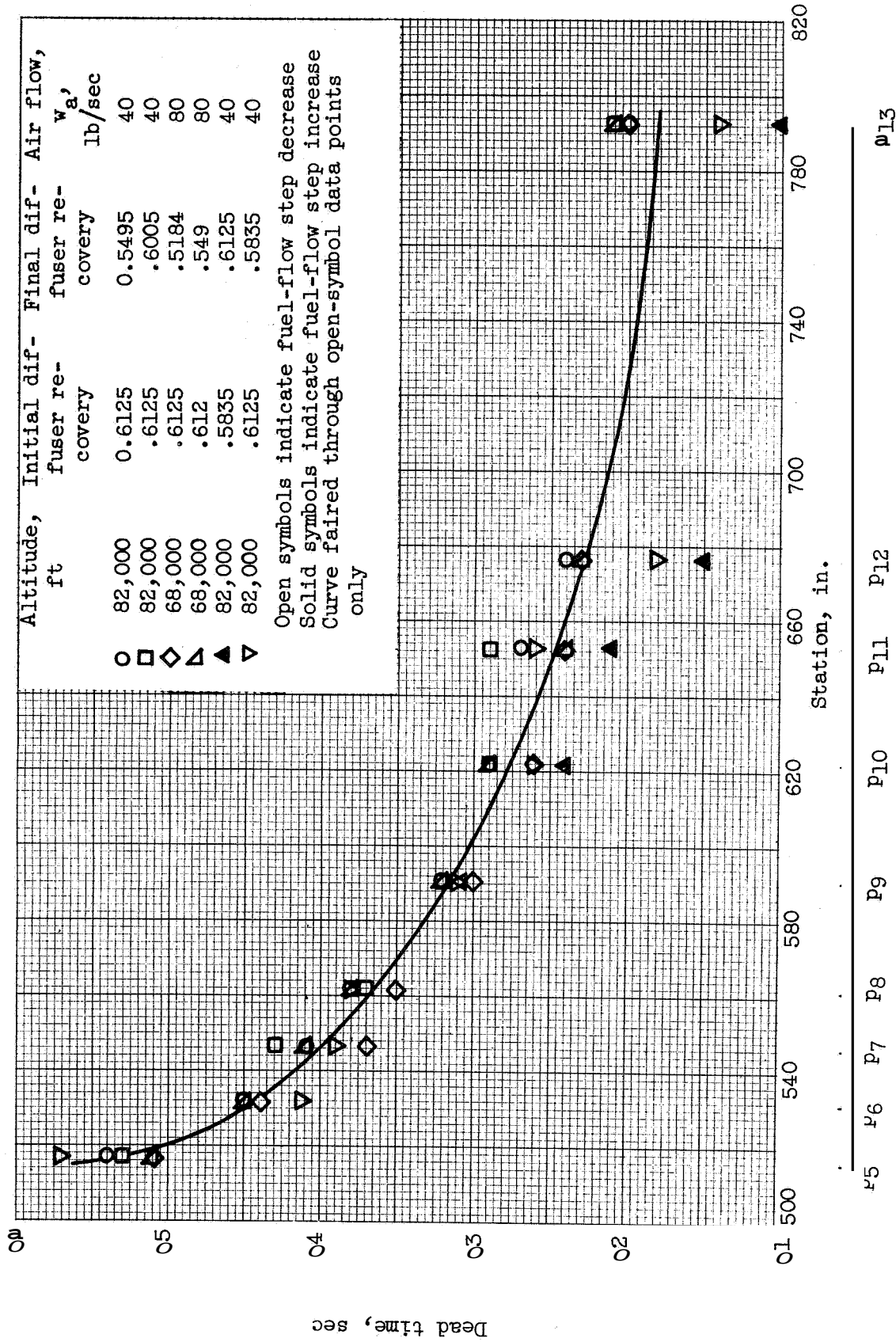


Figure 17. - Variation of dead time with distance from burning zone. Free-stream Mach number, 2.76; engine-inlet temperature, 5280 F.

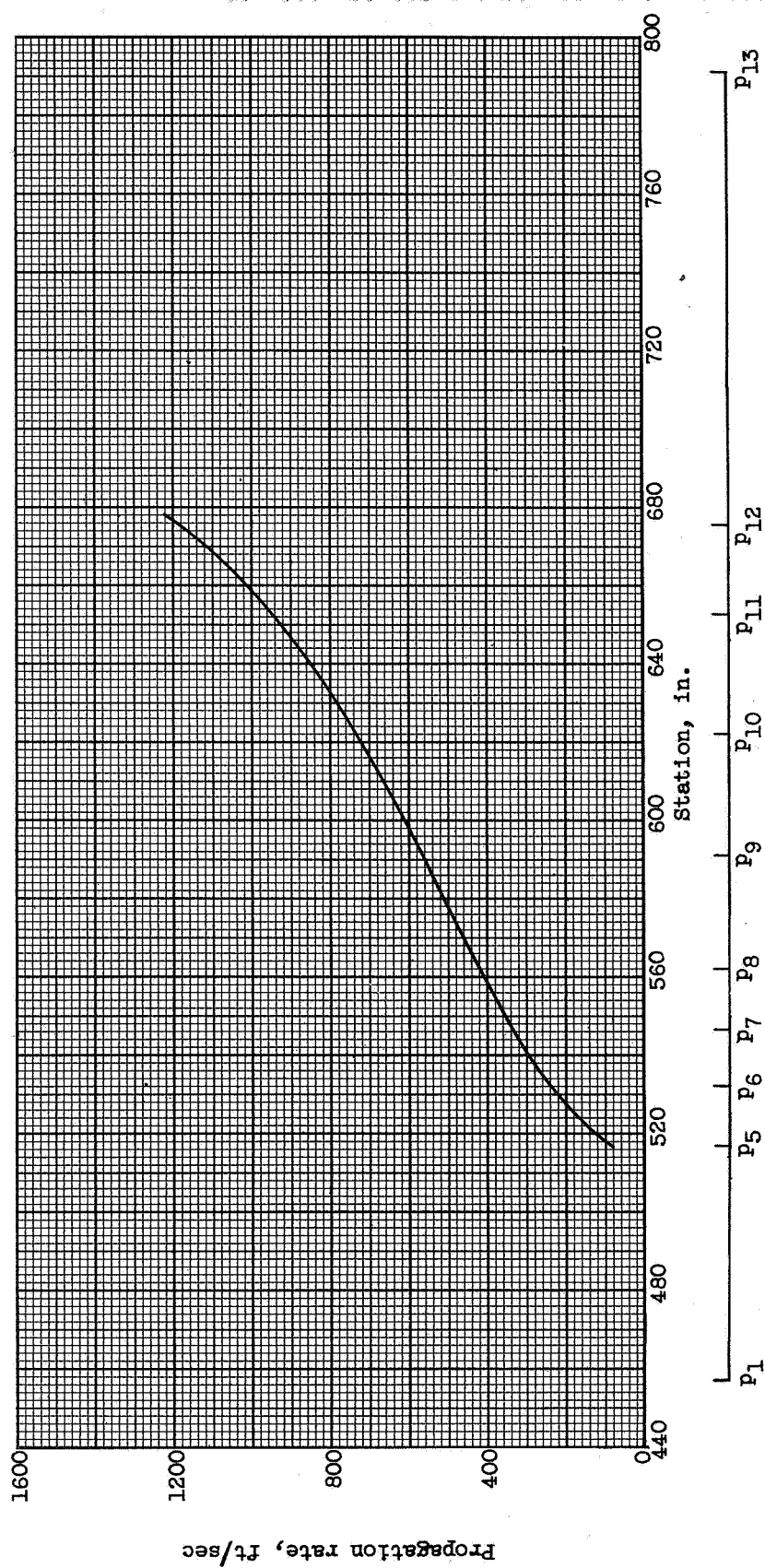
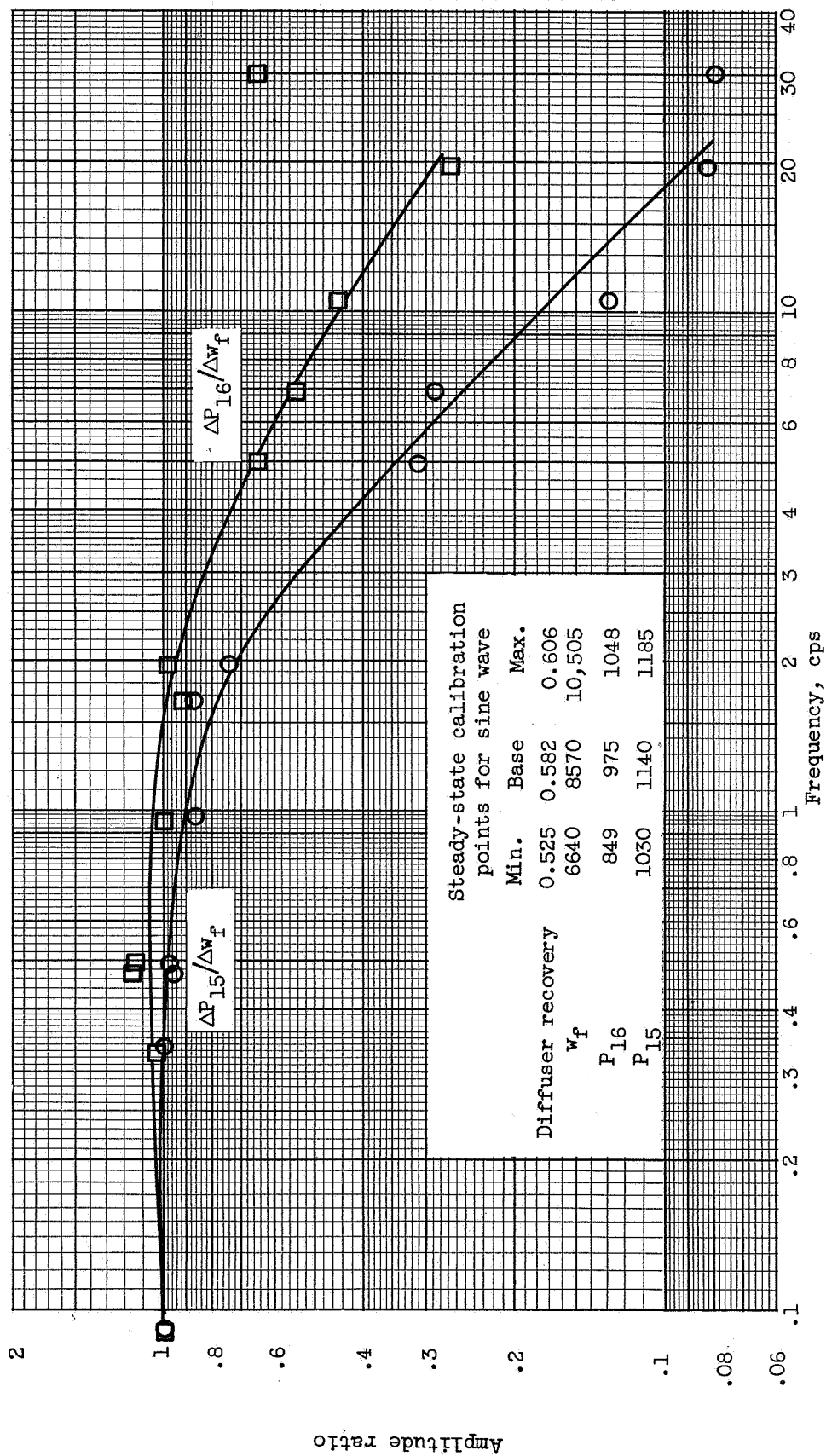
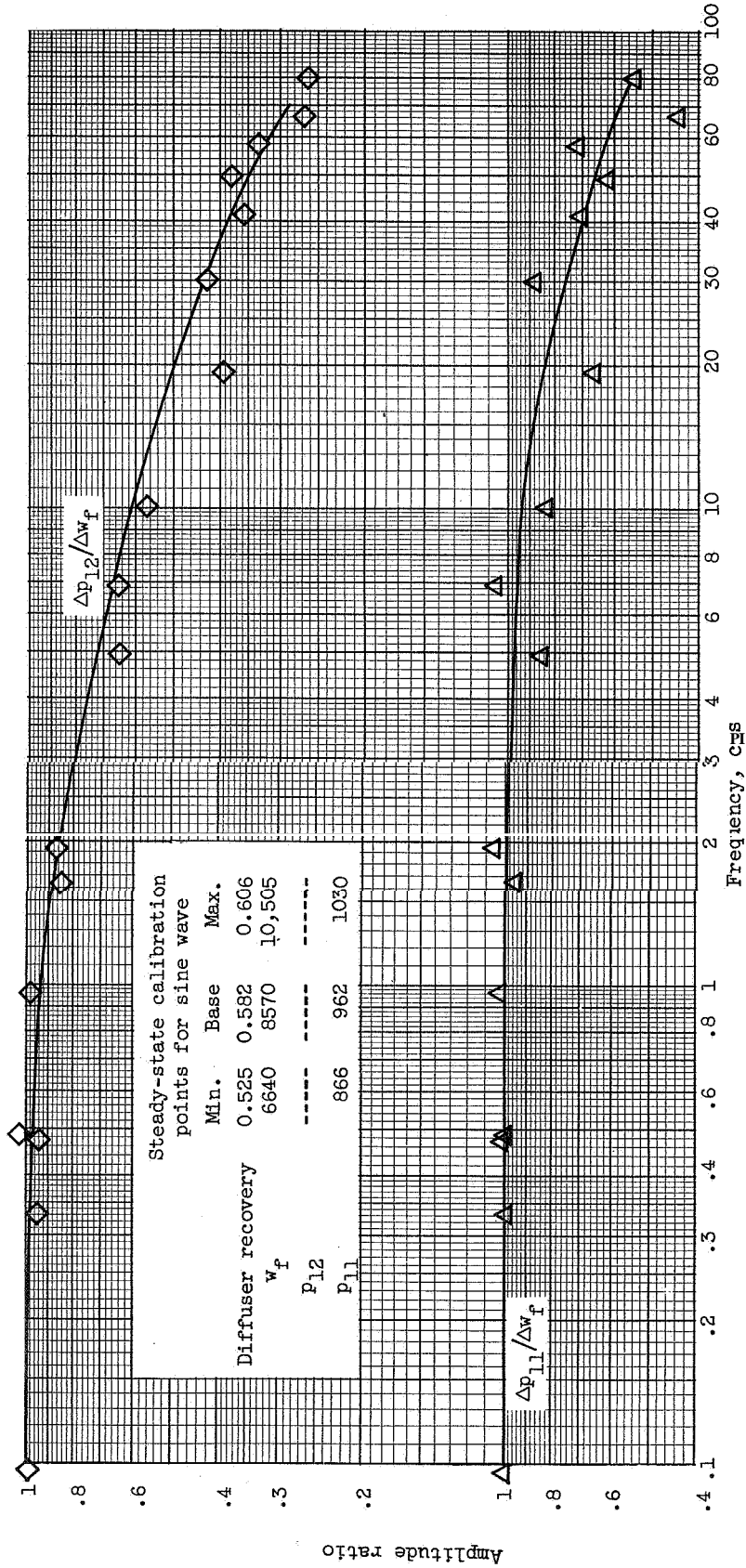


Figure 18. - Variation of propagation rate of pressure disturbance within diffuser. Free-stream Mach number, 2.76; engine-inlet temperature, 528° F.



(a) Amplitude ratio.

Figure 19. - Frequency response of engine pressures to fuel flow. Air flow, 60 pounds per second; free-stream Mach number, 2.76; engine-inlet temperature, 528° F.

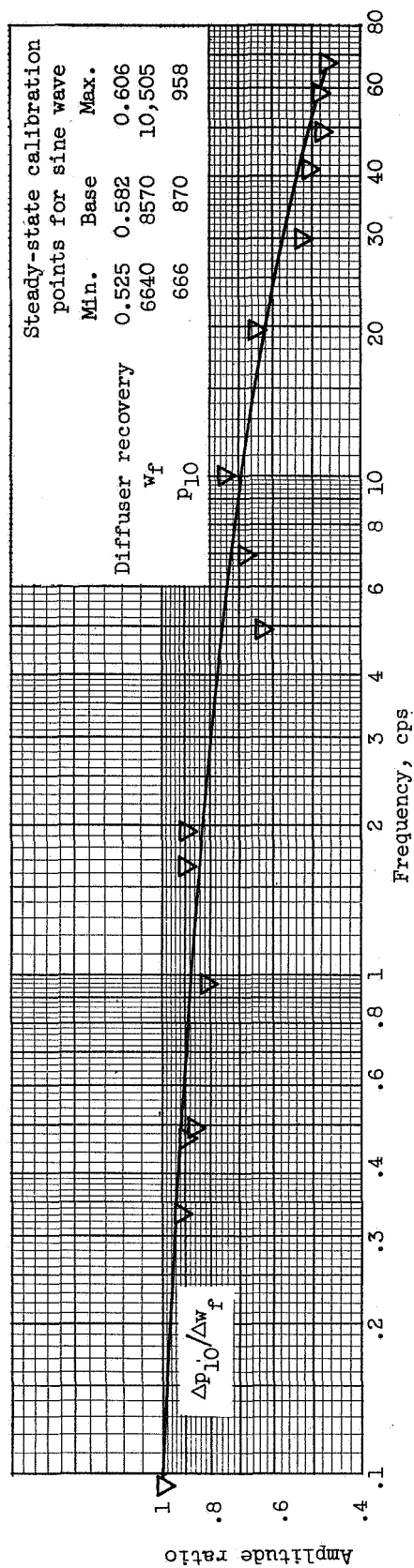


(a) Continued Amplitude ratio

Figure 19. - Continued. Frequency response of engine pressures to fuel flow. Air flow, 60 p nds per second; free-stream Mach number, 2.76; engine-inlet temperature, 528° F.

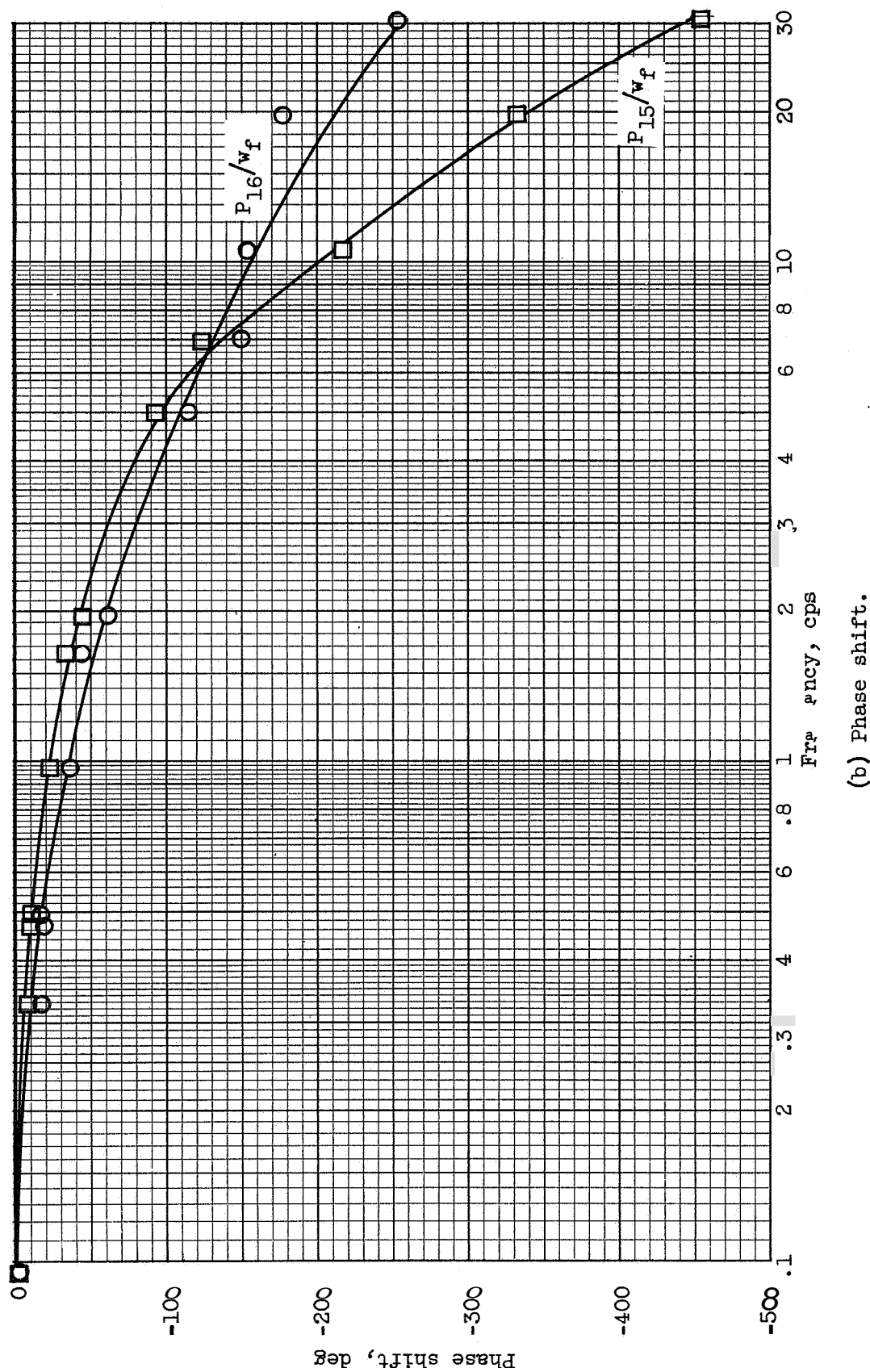
CONFIDENTIAL

NACA RM E55J12



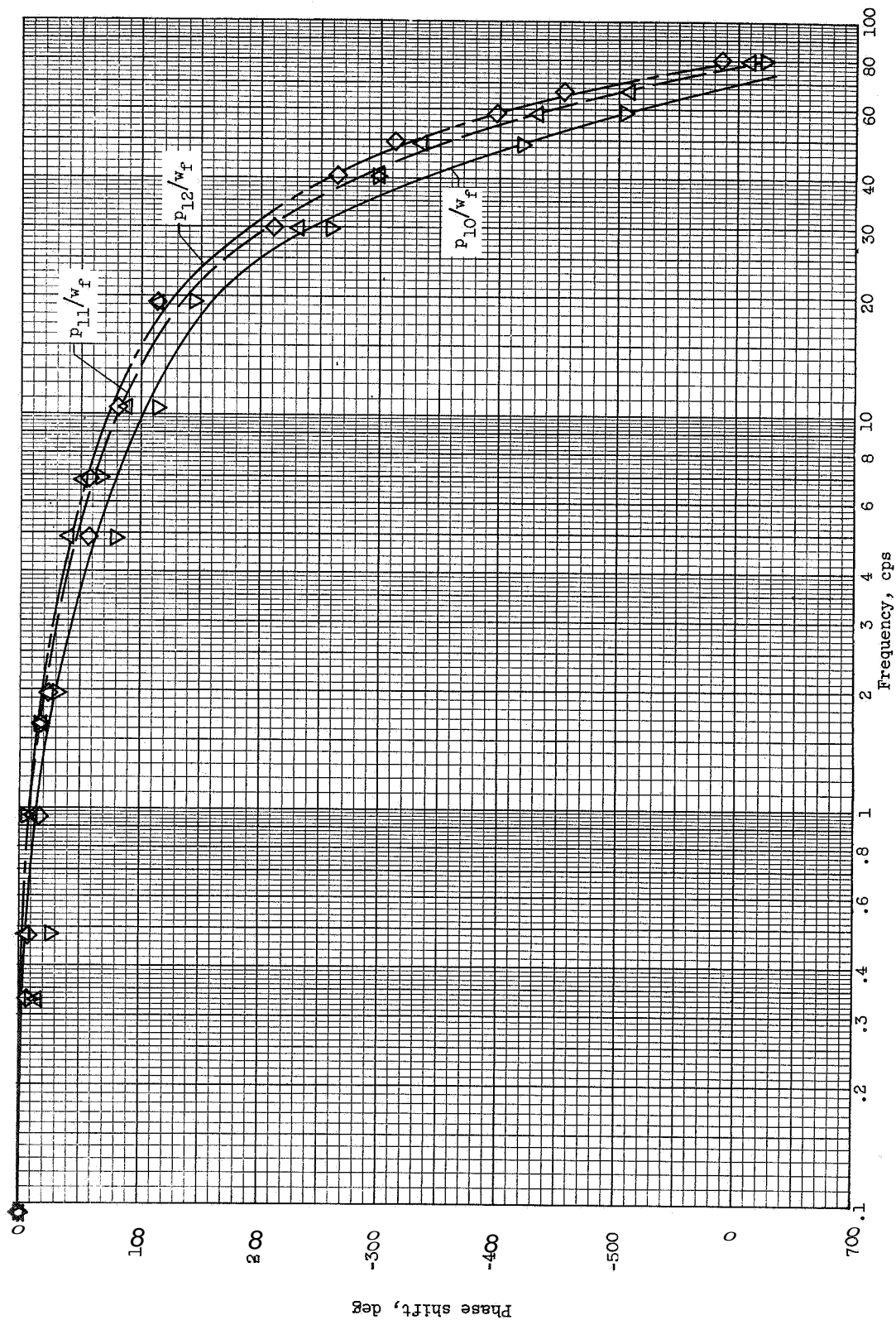
(a) Concluded. Amplitude ratio.

Figure 19. - Continued. Frequency response of engine pressures to fuel flow. Air flow, 60 pounds per second; free-stream Mach number, 2.76; engine-inlet temperature, 528° F.



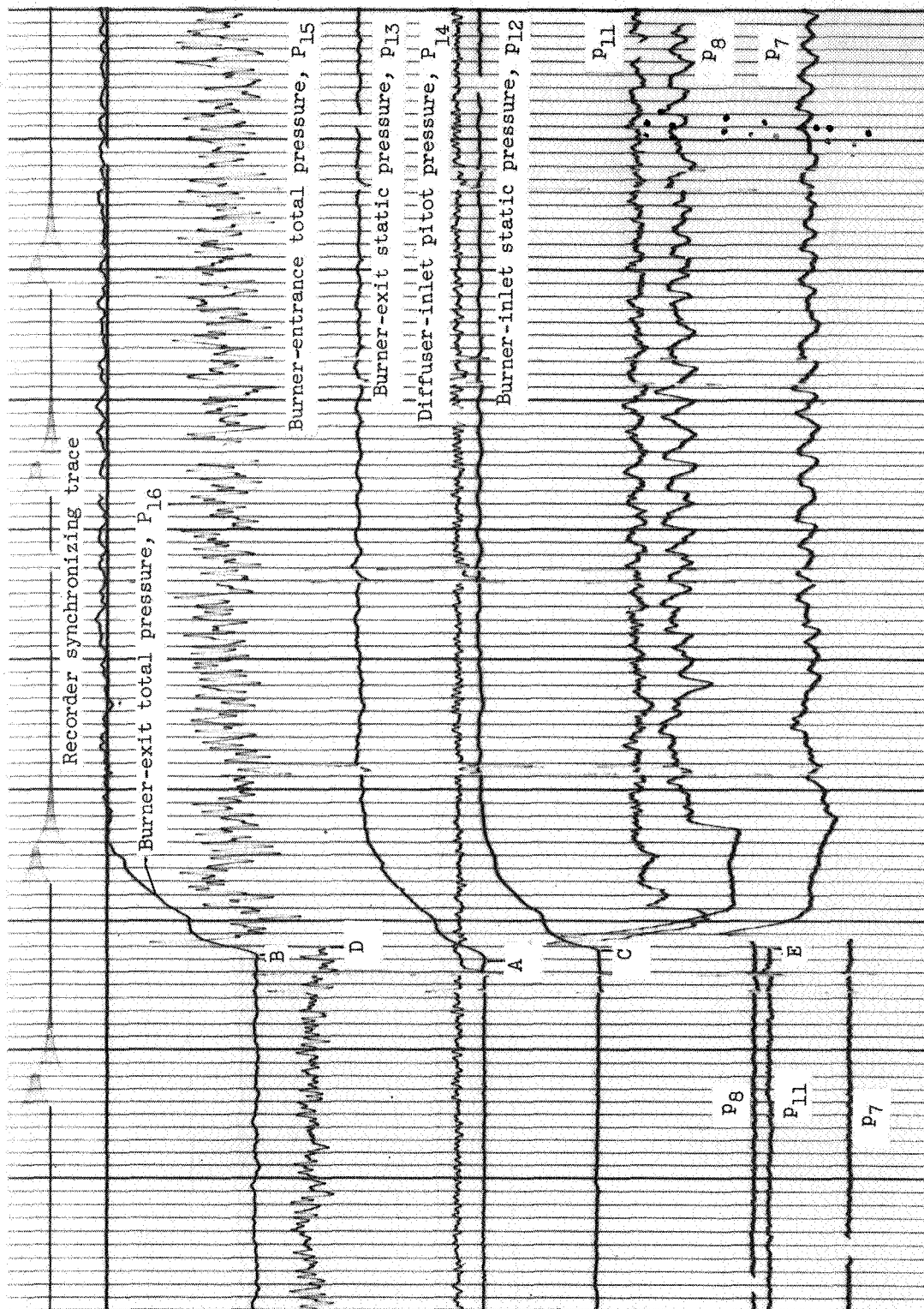
(b) Phase shift.

Figure 19. - Continued. Frequency response of engine pressures to fuel flow. Air flow, 60 pounds per second; free-stream Mach number, 2.76; engine-inlet temperature, 528° F.



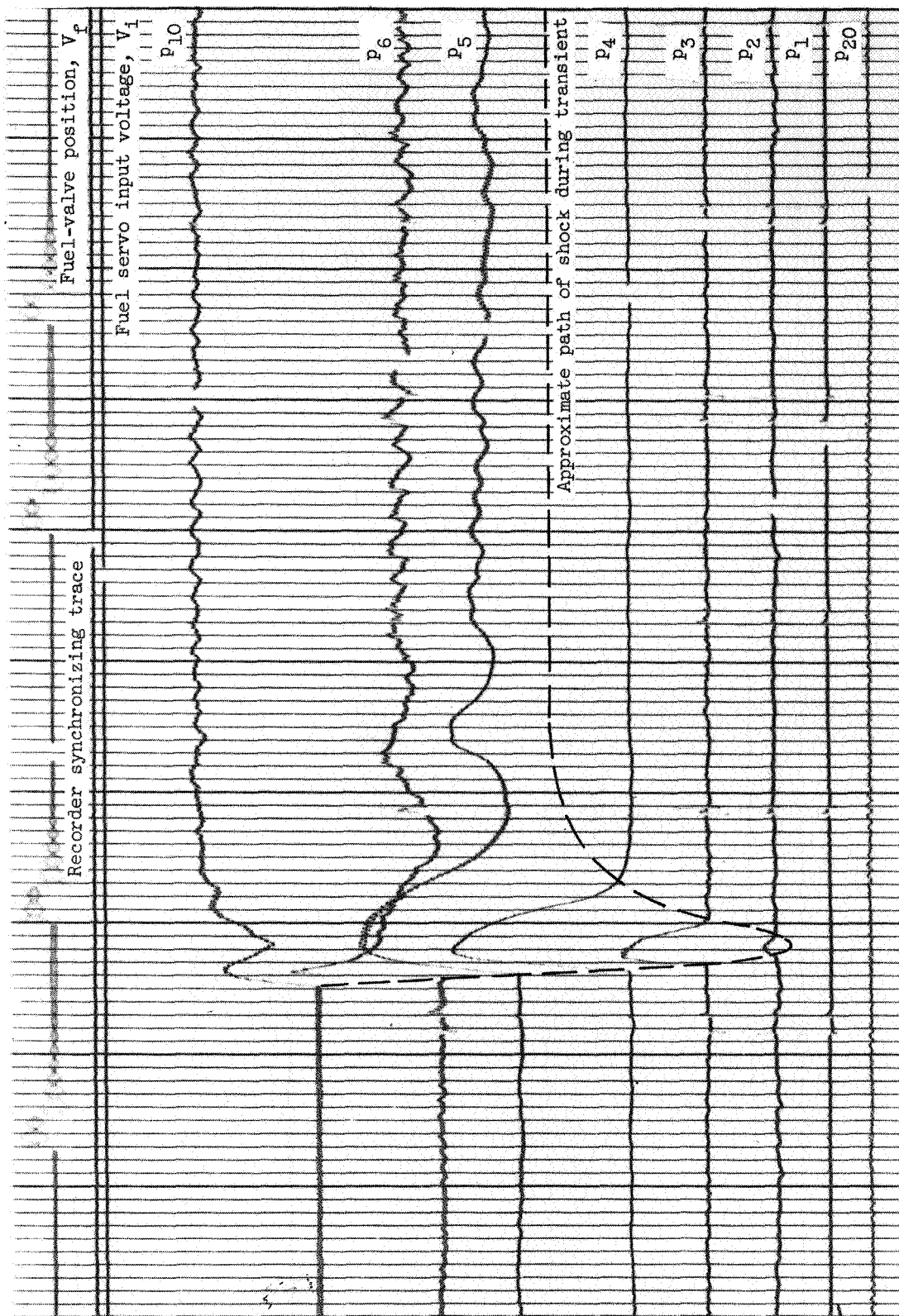
(b) Concluded. Phase shift.

Figure 19. - Concluded. Frequency response of engine pressures to fuel flow. Air flow, 60 pounds per second; free-stream Mach number, 2.76; engine-inlet temperature, 528° F.



(a) Recorder 1.

Figure 20. - Response of engine and diffuser pressures during an ignition transient. Fuel-air ratio, 0.0515; altitude, 68,000 feet; free-stream Mach number, 2.76; engine-inlet temperature, 528° F.



(b) Recorder 2.

Figure 20. - Concluded. Response of engine and diffuser pressures during an ignition transient. Fuel-air ratio, 0.0515; altitude, 68,000 feet; free-stream Mach number, 2.76; engine-inlet temperature, 528° F.

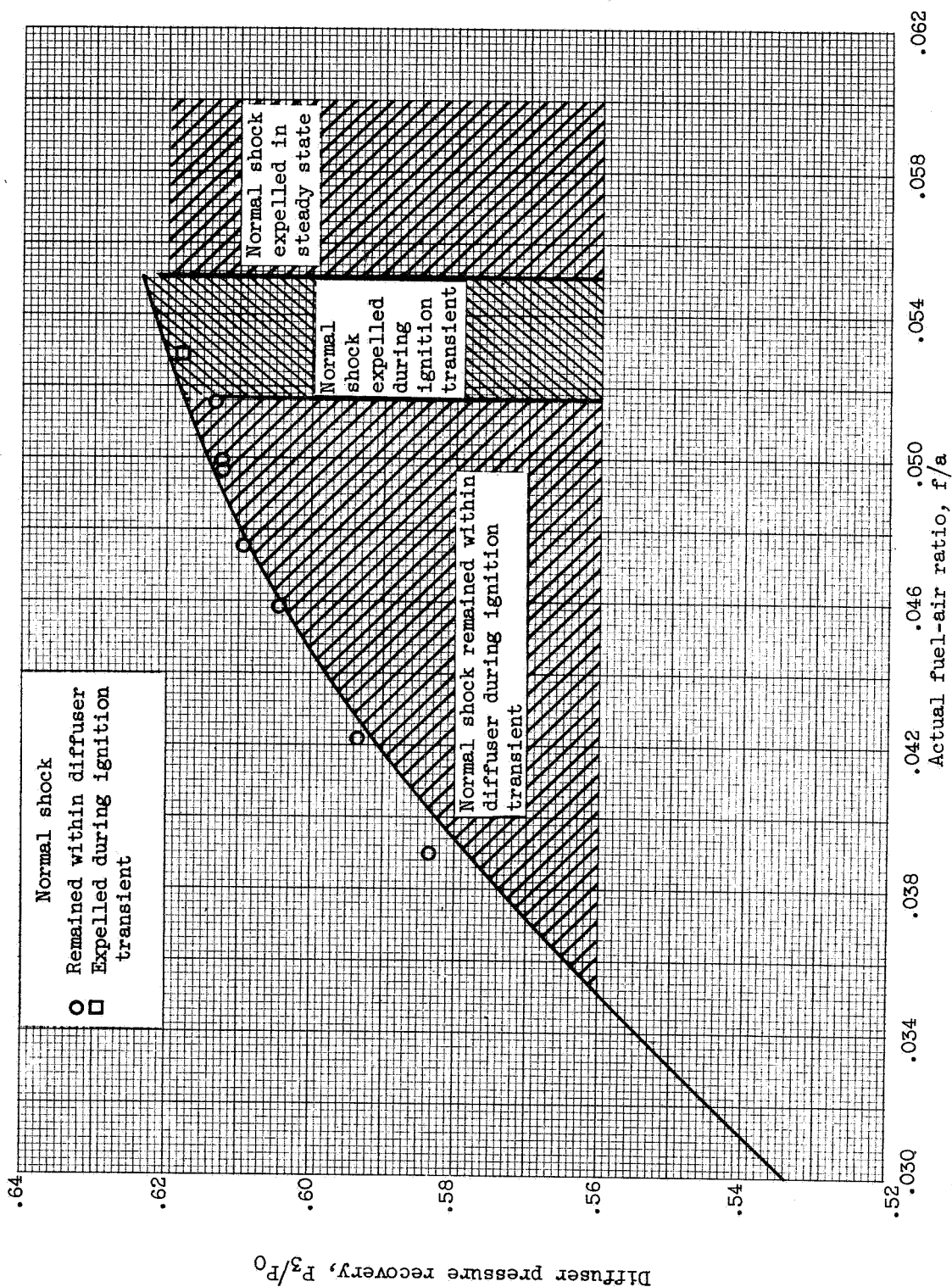


Figure 21. - Diffuser operation during ignition transient as affected by fuel-air ratio at ignition. Altitude, 68,000 feet; air flow, 80 pounds per second; free-stream Mach number, 2.76; engine-inlet temperature, 5280 F.

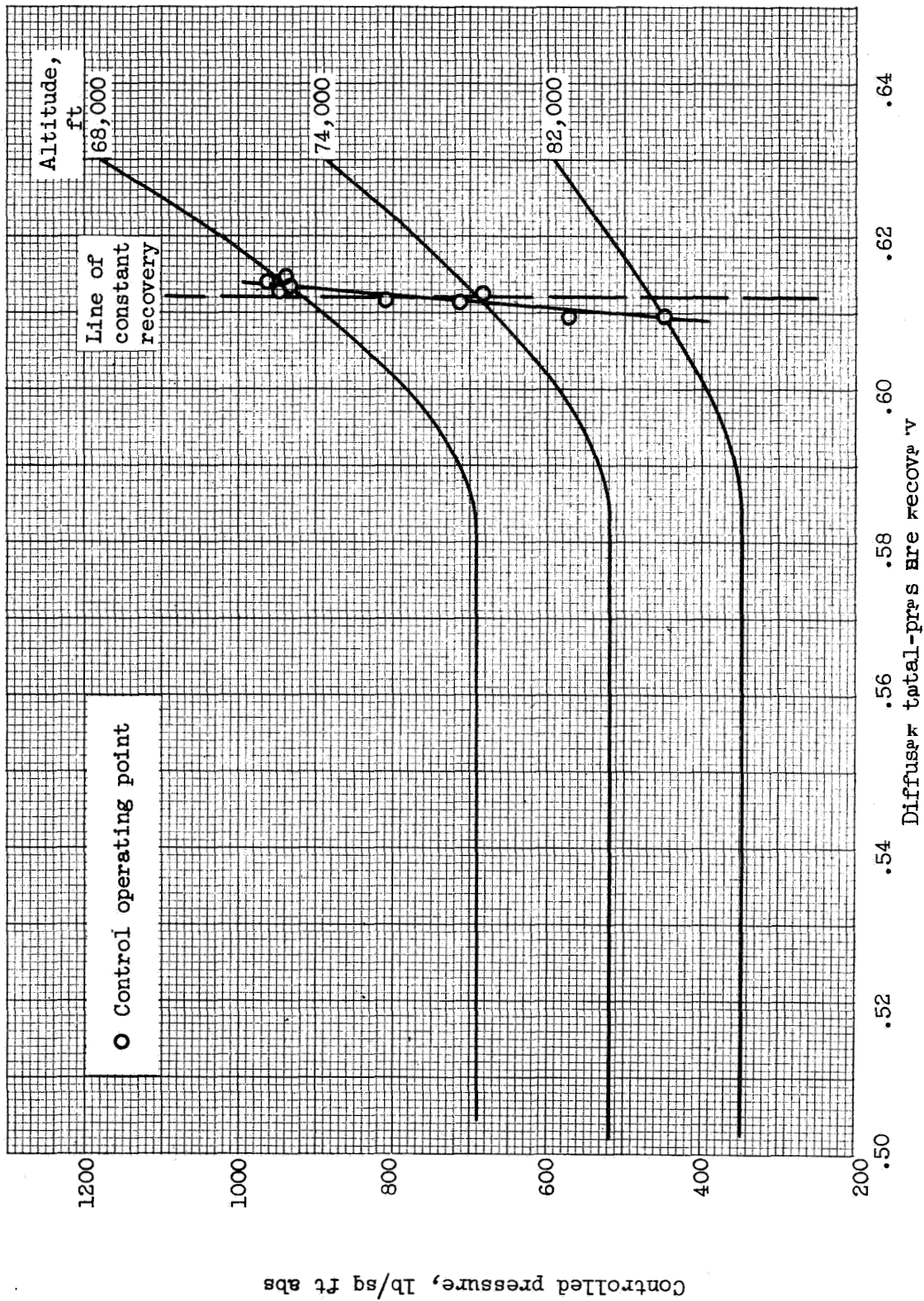
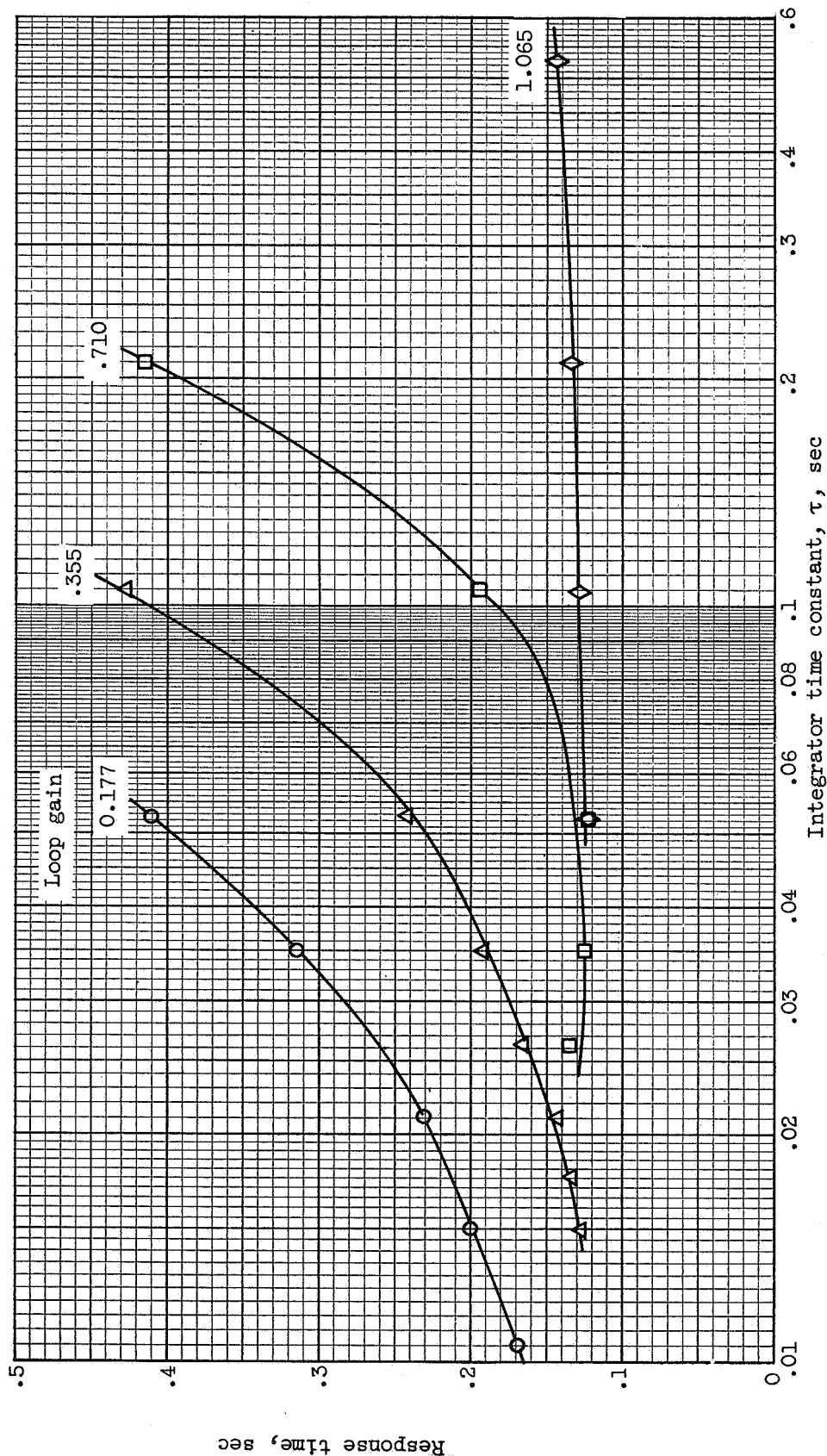
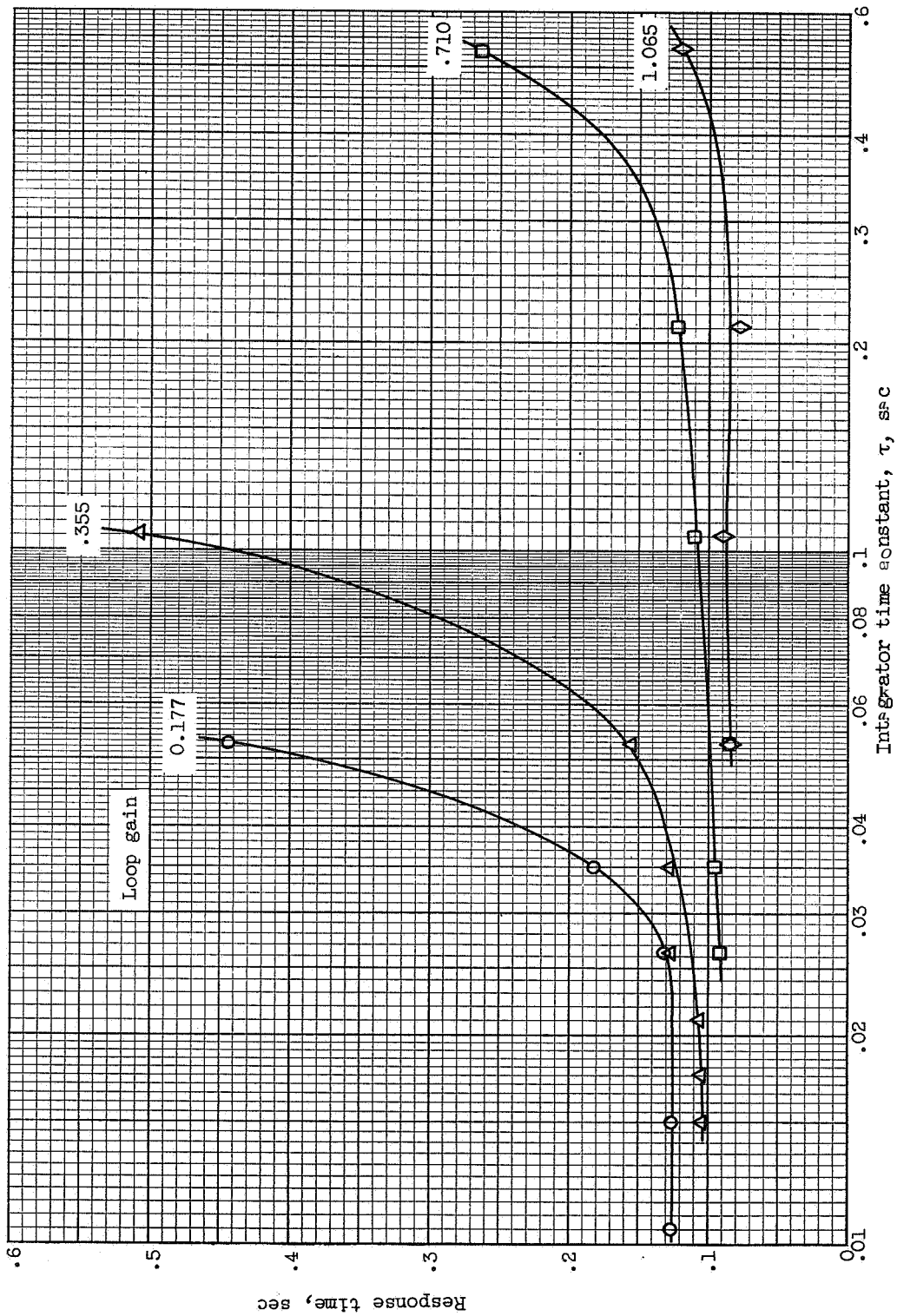


Figure 22. - Steady-state performance of P532 control over range of altitudes. Free-stream Mach number, 2.76; engine-inlet temperature, 528° F.



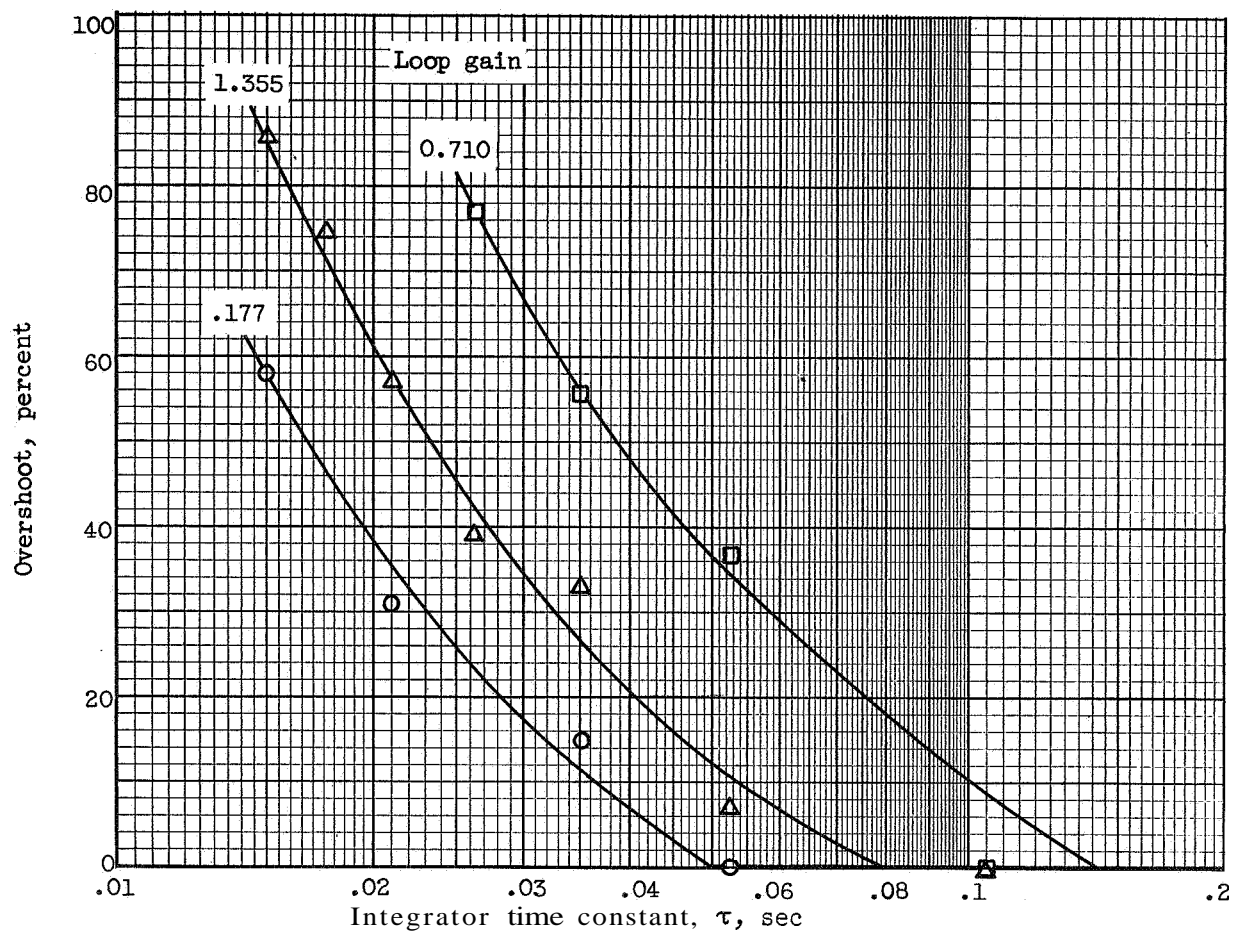
(a) Step increase in fuel flow of 2130 pounds per hour.

Figure 23. - Effect of integrator time constant on response time for various loop gains. Controlled parameters are, p532; altitude, 68,000 feet; air flow, 80 pounds per second; engine gain, 0.090 (lb/sq ft)/(lb/hr); free-stream Mach number, 2.76; engine-inlet temperature, 528° F.



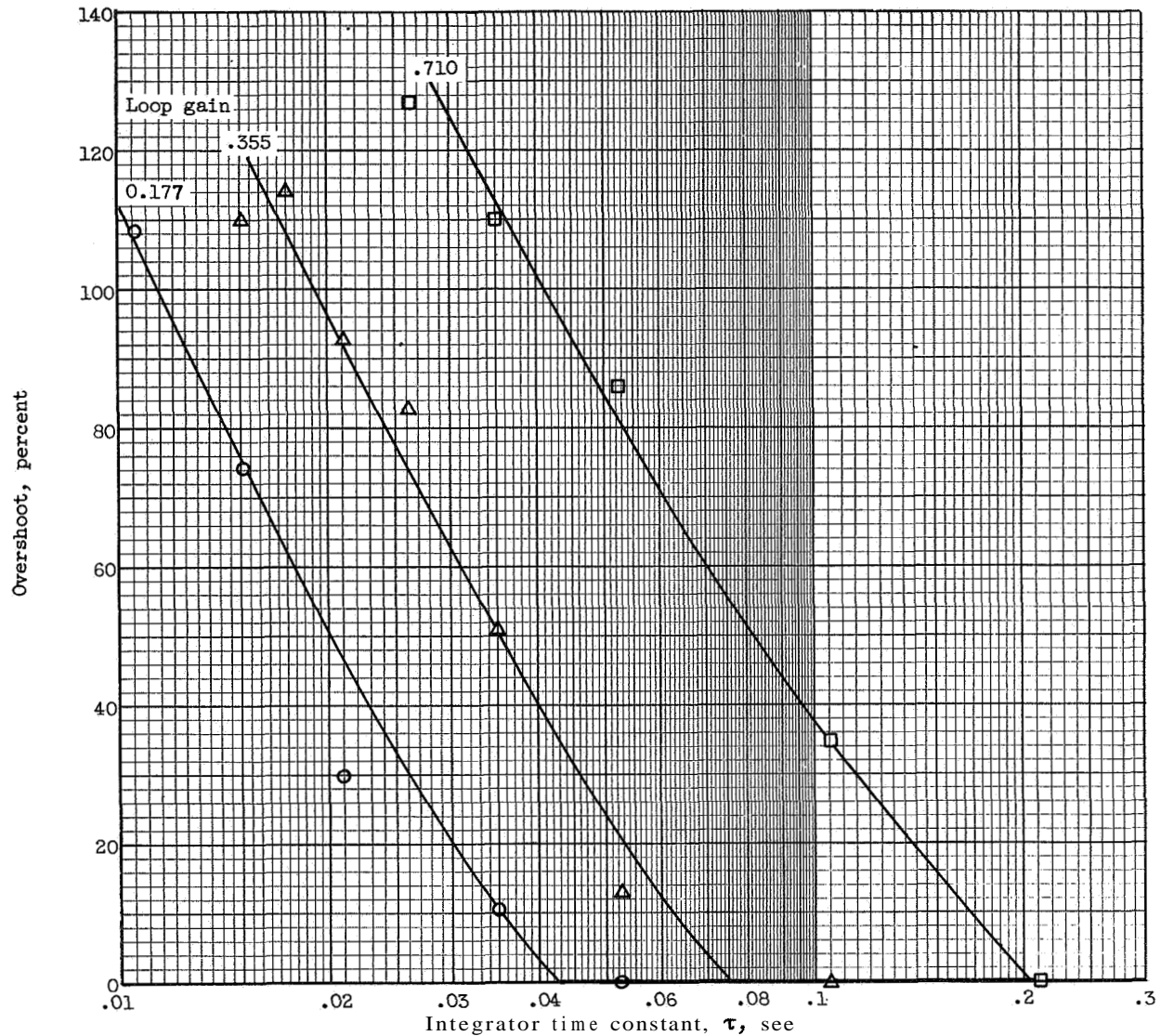
(b) Step decrease in fuel flow of ZL30 pounds per hour

Figure 23. - Concluded. Effect of integrator time constant on response time for various loop gains. Controlled pressure, P<sub>532</sub>; altitude, 68,000 feet; air flow, 80 pounds per second; engine gain, 0.090(lb/sq ft)/(lb/hr); free-stream Mach number, 2.76; engine-inlet temperature, 5280 F.



(a) Step increase in fuel flow of 2130 pounds per hour.

Figure 24. - Effect of integrator time constant on percent overshoot for various loop gains. Controlled pressure,  $P_{532}$ ; altitude, 68,000 feet; air flow, 80 pounds per second; engine gain,  $0.090(\text{lb}/\text{sq ft})/(\text{lb}/\text{hr})$ ; free-stream Mach number, 2.76; engine-inlet temperature, 520° F.



(b) Step decrease in fuel flow of 2130 pounds per hour.

Figure 24. - Concluded. Effect of integrator time constant on percent overshoot for various loop gains. Controlled pressure,  $P_{532}$ ; altitude, 68,000 feet; air flow, 80 pounds per hour; engine gain,  $0.090(\text{lb/sq ft})/(\text{lb/hr})$ ; free-stream Mach number, 2.76; engine-inlet temperature,  $528^\circ\text{F}$ .

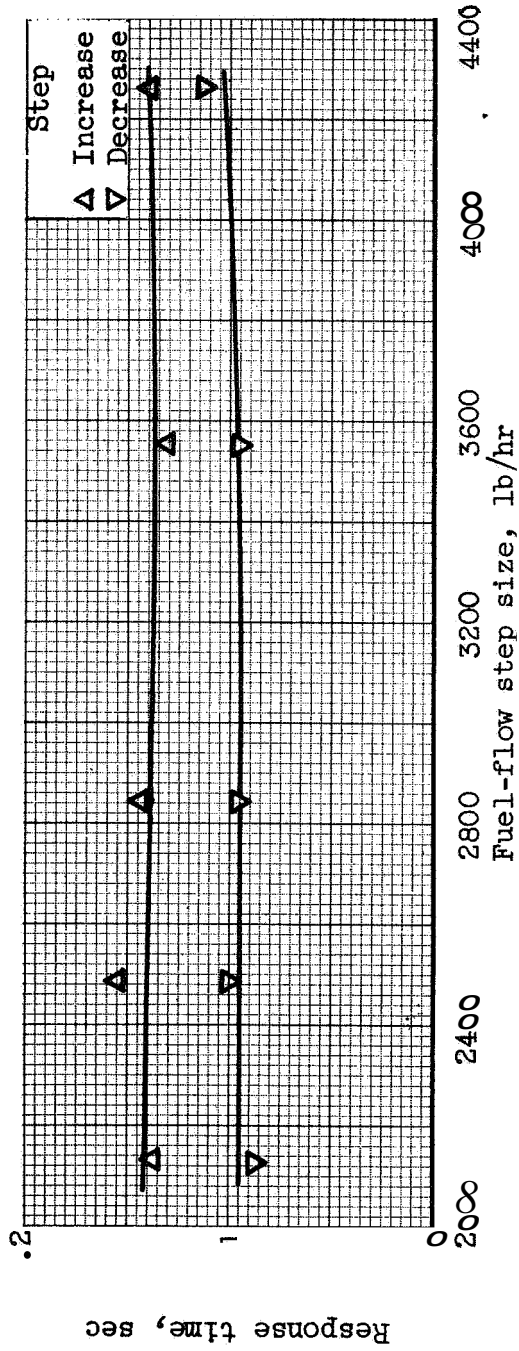


Figure 25. - Effect of step size on response time for c stage control settings. Controlled pressure, P532; air flow, 80 pounds per second; loop gain, 0.710; integrator time constant, 0.035 second; free-stream Mach number, 2.76; engine-inlet temperature, 528° F.

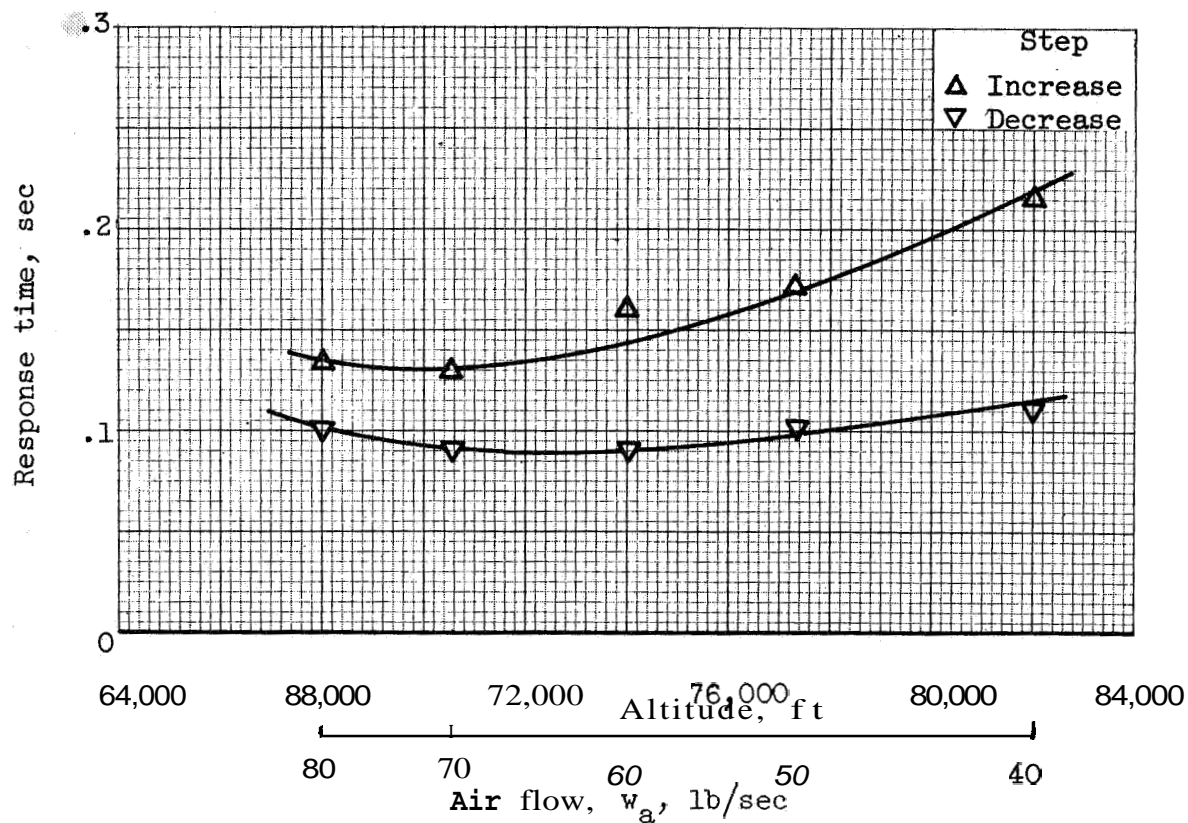


Figure 26. - Effect of altitude on response time for constant control settings. Controlled pressure,  $p_{532}$ ; air flow, 80 pounds per second; loop gain, 0.710; engine gain, 0.090 (lb/sq ft)/(lb/hr); integrator time constant, 0.0525 second; step size, 0.0074 in fuel-air ratio; free-stream Mach number, 2.76; engine-inlet temperature, 528° F.

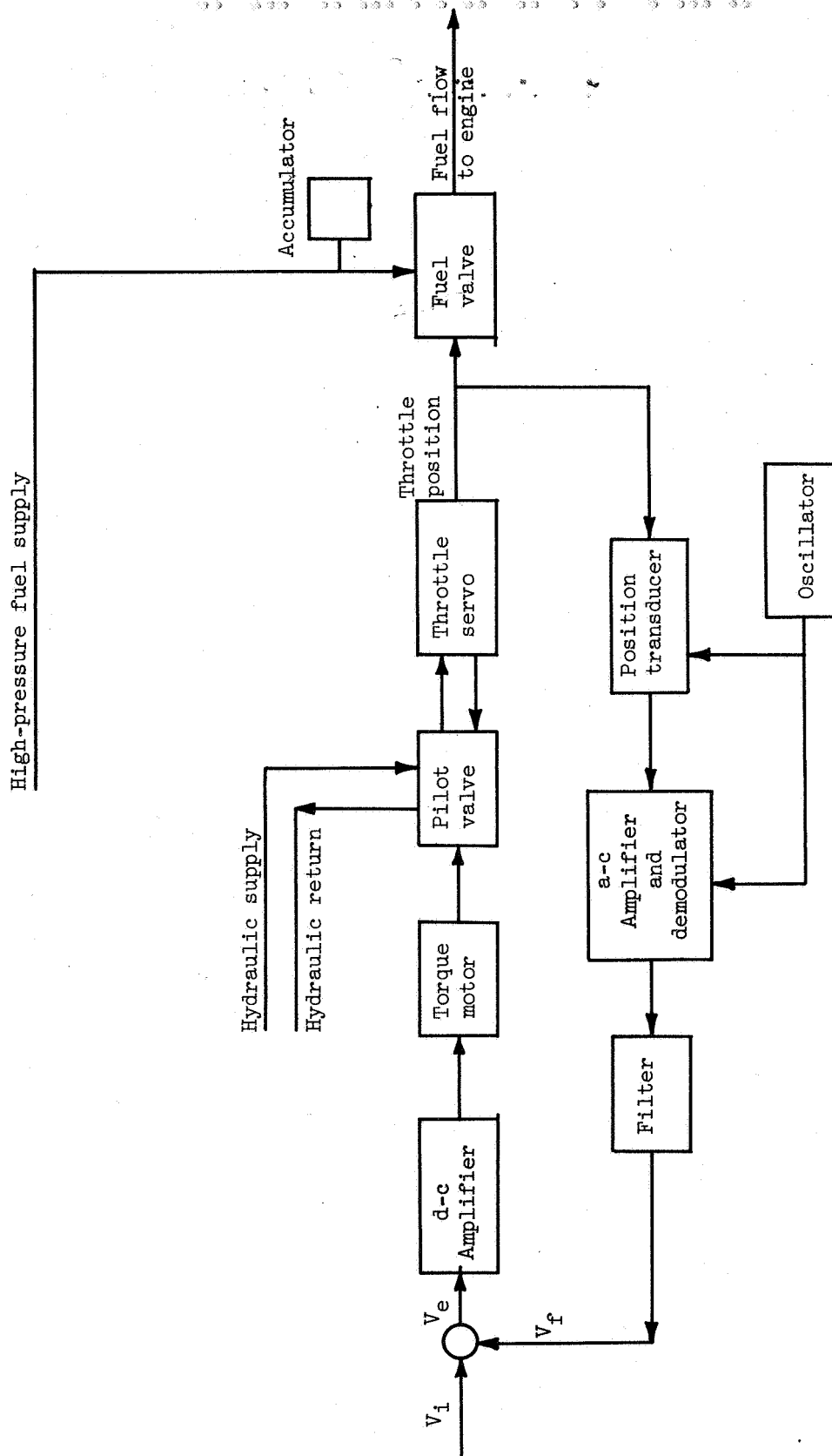


Figure 27. - Block diagram of fuel system used for engine dynamics and controls investigation.